



Contents lists available at ScienceDirect

Metabolism Clinical and Experimental

journal homepage: www.metabolismjournal.com

Diet and exercise reduce pre-existing NASH and fibrosis and have additional beneficial effects on the vasculature, adipose tissue and skeletal muscle via organ-crosstalk



Anita M. van den Hoek^{a,*}, Jelle C.B.C. de Jong^{a,b}, Nicole Worms^a, Anita van Nieuwkoop^a, Marijke Voskuilen^a, Aswin L. Menke^a, Serene Lek^c, Martien P.M. Caspers^d, Lars Verschuren^d, Robert Kleemann^{a,e}

^a Department of Metabolic Health Research, The Netherlands Organization for Applied Scientific Research (TNO), Leiden, the Netherlands

^b Human and Animal Physiology, Wageningen University, Wageningen, the Netherlands

^c Cinnovate Health UK Ltd, Glasgow, United Kingdom

^d Department of Microbiology and Systems Biology, The Netherlands Organization for Applied Scientific Research (TNO), Zeist, the Netherlands

^e Department of Vascular Surgery, Leiden University Medical Center, Leiden (LUMC), the Netherlands

ARTICLE INFO

Article history:

Received 19 May 2021

Accepted 28 August 2021

Available online xxxx

Keywords:

NAFLD

Fibrosis

Atherosclerosis

Lifestyle interventions

WAT-liver axis

Muscle-liver axis

ABSTRACT

Background: Non-alcoholic steatohepatitis (NASH) has become one of the most common liver diseases and is still without approved pharmacotherapy. Lifestyle interventions using exercise and diet change remain the current treatment of choice and even a small weight loss (5–7%) can already have a beneficial effect on NASH. However, the underlying molecular mechanisms of exercise and diet interventions remain largely elusive, and it is unclear whether they exert their health effects via similar or different pathways.

Methods: *Ldlr*^{−/−}.Leiden mice received a high fat diet (HFD) for 30 weeks to establish a severe state of NASH/fibrosis with simultaneous atherosclerosis development. Groups of mice were then either left untreated (control group) or were treated for 20 weeks with exercise (running wheel), diet change (switch to a low fat chow diet) or the combination thereof. The liver and distant organs including heart, white adipose tissue (WAT) and muscle were histologically examined. Comprehensive transcriptome analysis of liver, WAT and muscle revealed the organ-specific effects of exercise and diet and defined the underlying pathways.

Results: Exercise and dietary change significantly reduced body weight, fat mass, adipocyte size and improved myosteatosis and muscle function with additive effects of combination treatment. WAT inflammation was significantly improved by diet change, tended to be reduced with exercise, and combination therapy had no additive effect. Hepatic steatosis and inflammation were almost fully reversed by exercise and diet change, while hepatic fibrosis tended to be improved with exercise and was significantly improved with diet change. Additive effects for the combination therapy were shown for liver steatosis and associated liver lipids, and atherosclerosis, but not for hepatic inflammation and fibrosis. Pathway analysis revealed complementary effects on metabolic pathways and lipid handling processes, thereby substantiating the added value of combined lifestyle treatment.

Conclusions: Exercise, diet change and the combination thereof can reverse established NASH/fibrosis in obese *Ldlr*^{−/−}.Leiden mice. In addition, the lifestyle interventions had beneficial effects on atherosclerosis, WAT inflammation and muscle function. For steatosis and other parameters related to adiposity or lipid metabolism, exercise and dietary change affected more distinct pathways that acted complementary when the interventions were combined resulting in an additive effect for the combination therapy on important endpoints including NASH and atherosclerosis. For inflammation, exercise and diet change shared several underlying pathways resulting in a net similar effect when the interventions were combined.

© 2021 The Author(s). Published by Elsevier Inc. This is an open access article under the CC BY-NC-ND license (<http://creativecommons.org/licenses/by-nc-nd/4.0/>).

Abbreviations: ALT, alanine aminotransferase; AMPK, AMP-activated protein kinase; DEP, differentially expressed pathways; DHA, docosahexaenoic acid; FDR, false discovery rate; FPLC, fast-performance liquid chromatography; GEO, gene expression omnibus; H&E, haematoxylin and eosin; HFD, high fat diet; HOMA-IR, homeostasis model assessment for insulin resistance; HPS, haematoxylin-phloxine-saffron; LXR, liver X receptor; MMP1, downregulating matrix metalloproteinase 1; MRI, magnetic resonance imaging; NAFLD, non-alcoholic fatty liver disease; NASH, non-alcoholic steatohepatitis; PPAR, peroxisome proliferator-activated receptor; RXR, retinoid X receptor; SAA, serum amyloid A; SEM, standard error of the mean; SHG, Second Harmonic Generation; SREBP-1, sterol regulatory element-binding protein-1; TCA, tricarboxylic acid cycle; TGF- β , transforming growth factor β ; TIMP-1, tissue inhibitor of metalloproteinase 1; TNF- α , tumour necrosis factor α ; UR, upstream regulator; WAT, white adipose tissue.

* Corresponding author at: TNO Metabolic Health Research, Zernikedreef 9, 2333 CK Leiden, the Netherlands.

E-mail address: a.vandenhoek@tno.nl (A.M. van den Hoek).

<https://doi.org/10.1016/j.metabol.2021.154873>

0026-0495/© 2021 The Author(s). Published by Elsevier Inc. This is an open access article under the CC BY-NC-ND license (<http://creativecommons.org/licenses/by-nc-nd/4.0/>).

1. Introduction

Non-alcoholic fatty liver disease (NAFLD) is considered to be the manifestation of the metabolic syndrome in the liver and has emerged as the most prevalent form of chronic liver disease worldwide. Non-alcoholic steatohepatitis (NASH) is a severe form of NAFLD, characterized by the accumulation of fat in the liver (steatosis) in concert with inflammation, which can progress to liver fibrosis and cirrhosis [1]. The disease is closely related to obesity, insulin resistance and dyslipidemia, and similar as for the metabolic syndrome, has been associated with an increased risk of developing diabetes or cardiovascular disease [2–4]. Due to the increased prevalence, there exists a great need to develop new NASH therapeutics. However, to date no single pharmacotherapy has been approved for the treatment of NASH, and lifestyle recommendations on diet and exercise remain the current treatment [4,5].

Lifestyle modifications, although difficult to maintain, have been shown by several studies to be very successful in combatting NASH ([6–10] and reference herein). The degree of weight loss is typically related to the improvement of histological NASH parameters [6,8,10], and even a small reduction in body weight (5–7%) can already have a beneficial effect on NASH [8,10]. It is not completely clear how a relatively small reduction in body weight can affect the histological features of NASH in the liver. NASH is a complex multifactorial disease in which dysregulation of the metabolic homeostasis in liver as well as in distant organs may play a large role. The molecular mechanisms that underly both healthy and pathological metabolic states are still being elucidated and multiple metabolically active organs such as liver, white adipose tissue (WAT) and muscle interact [11]. Animal studies can be most helpful to provide more insight into this inter-organ cross-talk and the mechanistic pathways underlying NASH development and should pave the way towards the development of lifestyle modification guidelines on which future pharmacotherapies should be based upon [12].

In the present study we investigated the effect of lifestyle interventions on NASH in *Ldlr*^{−/−}.Leiden mice, a well-established model for hyperlipidemia and atherosclerosis that develop NASH with advanced fibrosis when fed a high fat diet [13–22]. The model has been proven to be responsive to several nutritional and pharmacological interventions [15,17,18,20,21,23–25]. In this particular study, mice with a severe state of NASH and atherosclerosis were treated with exercise, diet change or the combination thereof. Histological examination of liver, WAT and muscle was used to investigate the organ-specific effects of the exercise and diet interventions, as well as their putative additive effect. Transcriptome analysis on all three tissues was subsequently used to investigate in more detail the intervention-specific and organ-specific effects, as well as the underlying pathways and possible interactions between the different organs that ultimately all may affect NASH and atherosclerosis.

2. Material and methods

2.1. Animals and experimental design

All animal care and experimental procedures were approved by the Ethical Committee on Animal Care and Experimentation (Zeist, The Netherlands; approval reference number TNO-312, Date 2 October 2017), and were in compliance with European Community specifications regarding the use of laboratory animals. Fourteen–sixteen weeks old male *Ldlr*^{−/−}.Leiden mice (TNO, Metabolic Health Research, Leiden, The Netherlands) were used. This substrain of the *Ldlr*^{−/−} mouse has a 94% C57BL/6 J background and 6% 129S1/SvImJ background. Mice were group housed in a temperature-controlled room on a 12 hour light-dark cycle and had free access to food and heat sterilized water. Mice were first matched on age, body weight, blood glucose, plasma cholesterol and triglycerides into two groups of mice: mice (n = 10; healthy reference group) that were kept on a grain-based low (9%) fat chow diet (R/M-H chow, Ssniff Spezialdiäten

GmbH, Soest, Germany) or mice (n = 60) that were given a high fat diet (HFD) containing 45 kcal% fat from lard, 35 kcal% from carbohydrates and 20 kcal% casein (D12451, Research Diets, new Brunswick, NJ, USA) for 30 weeks to induce obesity, NASH and atherosclerosis. After 30 weeks mice that were allocated to the HFD group were matched another time for age, body weight, blood glucose, plasma cholesterol and triglycerides into four groups: mice that remained on the HFD for another 20 weeks (n = 17; HFD control group), mice that remained on HFD and received a running-wheel (Mouse Igloo+Fast Trac, Datesand, Bredbury, England) with unlimited access in their cage for voluntary activity (n = 17; exercise group), mice that were switched to the low fat chow diet (n = 18; dietary intervention group) and mice that received a running-wheel and were switched to low fat chow diet (n = 18; combination group). In addition to the aforementioned groups, an additional chow reference group (n = 9) and an additional HFD reference group (n = 10) were added that were sacrificed after 30 weeks of diet feeding to determine liver pathology as a start-of-intervention reference. Body weight and food intake were determined regularly during the study. At t = 49 weeks total fat mass was determined using a NMR Echo MRI whole body composition analyzer (EchoMRI 2-in-1, Echo Medical Systems LTD, Houston, TX, USA) and grip strength was determined using a grip force meter (TSE Systems GmbH, Bad Homburg, Germany) by placing mice with four limbs on a grid attached to a force gauge and steadily pulling the mice by their tails. Grip strength was defined as the maximum strength produced by the mouse before releasing the grid. On each occasion five trials were performed for each mouse with a 1-minute resting period between the trials. For each mouse the lowest and highest values were subsequently excluded and the average value of the remaining three trials was used to generate a final score per mouse. At t = 50 weeks mice were sacrificed unfasted using gradual-fill CO₂ asphyxiation. Terminal blood was collected through cardiac heart puncture to prepare EDTA plasma and livers, perigonadal and visceral white adipose tissue (WAT) and muscles (gastrocnemius and quadriceps) were collected, weighed and fixed in formalin and paraffin-embedded (lobus sinister medialis hepatis and lobus dexter medialis hepatis, left side perigonadal WAT, half of visceral WAT, left gastrocnemius and quadriceps) for histological analysis or (remaining liver lobes and visceral WAT, right side perigonadal WAT, right gastrocnemius and quadriceps) fresh-frozen in N₂ and subsequently stored at −80 °C for biochemical analysis and gene expression analysis. Hearts with aortic root area were collected, formalin-fixed and paraffin-embedded and used for histological analysis of atherosclerosis development.

2.2. Plasma and tissue biochemical analysis

Blood glucose was measured at the time of blood sampling using a hand-held glucometer (Freestyle Disectronic, Vianen, The Netherlands). Plasma cholesterol and triglycerides were determined using enzymatic assays (CHOD-PAP and GPO-PAP, respectively; Roche Diagnostics, Almere, The Netherlands). Plasma insulin was analysed by ELISA (Mercodia AB, Uppsala, Sweden). Homeostasis model assessment (HOMA) was used to calculate relative insulin resistance (IR). Five hours fasting plasma insulin and fasting blood glucose values were used to calculate IR, as follows: $IR = [\text{insulin (ng/mL)} \times \text{glucose (mM)}] / 22.5$. Plasma alanine aminotransferase (ALT) was measured using a spectrophotometric activity assay (Reflotron-Plus, Roche). Serum amyloid A (SAA) was analysed by ELISA (Thermo Fisher Scientific, Waltham, Massachusetts, USA), tumour necrosis factor- α (TNF- α) was analysed by mouse cytokine panel assay of Quanterix (Quanterix, Billerica, Massachusetts, USA). E-selectin, leptin and adiponectin were analysed using Duoset mouse ELISAs (R&D Systems, Minneapolis, Canada) according to manufacturer's instruction. Intrahepatic concentration of triglycerides, free cholesterol and cholesterol esters, as well as intramuscular triglycerides, was determined as described previously [26]. Briefly, approximately 50 mg of tissue was

homogenized in phosphate buffered saline and samples were taken for measurement of protein content. Lipids were extracted and separated by high performance thin layer chromatography (HPTLC) on silica gel plates. Lipid spots were stained with a colour reagent (5 g MnCl₂·4H₂O, 32 mL 95–97% H₂SO₄ added to 960 mL of CH₃OH:H₂O 1:1 v/v) and quantified using Image Lab software (version 5.2.1, Bio-Rad Laboratories B.V., Veenendaal, The Netherlands). Hepatic collagen content was determined by measuring hydroxyproline with a colorimetric assay, the Sensitive total collagen assay (Quickzyme, Leiden, The Netherlands), as a readout of liver fibrosis.

2.3. Histology

Liver samples (lobus sinister medialis hepatis and lobus dexter medialis hepatis) were collected (from non-fasted mice), fixed in formalin and paraffin embedded, and 3 µm sections were stained with haematoxylin and eosin (H&E) and Sirius Red. NASH was scored blindly by a board-certified pathologist in H&E stained cross sections using an adapted grading system of human NASH [27,28]. In short, the level of macrovesicular and microvesicular steatosis was determined at 40× to 100× magnification relative to the total liver area analysed and expressed as a percentage. Inflammation was scored by counting the number of aggregates of inflammatory cells per field using a 100× magnification (view size of 4.2 mm²). The averages of five random non-overlapping fields were taken and values were expressed per mm². Hepatic fibrosis was identified using Sirius Red stained slides and evaluated by computerized image analysis of hepatic collagen content (as percentage of liver surface area and including blood vessels). In addition, the fibrosis stage was determined by a certified pathologist using the protocol of Tiniakos et al. [1], in which the presence of pathological collagen staining was scored as either absent (F0), observed within perisinusoidal/perivenular or periportal area (F1), within both perisinusoidal and periportal areas (F2), bridging fibrosis (F3) or cirrhosis (F4).

Hearts were fixed in formalin, embedded in paraffin and were sectioned perpendicular to the axis of the aorta. Serial cross sections (5 µm thick with intervals of 50 µm) were stained with haematoxylin-phloxine-saffron (HPS) for histological analysis. The average total lesion area per cross section was then calculated [29,30]. For determination of lesion severity, the lesions were classified into five categories according to the American Heart Association classification [31]: 0) no lesion, I) early fatty streak, II) regular fatty streak, III) mild plaque, IV) moderate plaque, and V) severe plaque.

Perigonadal and visceral WAT samples were collected, fixed in formalin and paraffin embedded, and 5 µm sections were stained with HPS for quantification of adipocyte size and inflammation using 3 randomly selected fields (1.56 mm² for perigonadal WAT and 0.56 mm² for visceral WAT). Adipocytes size was measured using the free software ImageJ and Adiposoft macros [32]. Adipose tissue inflammation was measured by counting crown-like structures (CLS) per field using a 100× magnification and values were expressed as number of CLS per 1000 adipocytes.

Quadriceps were collected, fixed in formalin and paraffin embedded, and 5 µm sections were immunolabeled by means of 1-hour incubation in 1/50 mouse anti-fast myosin antibody (A4335; Sigma-Aldrich) and developed using a red alkaline phosphatase substrate kit (SK5100; Vector) to reveal the overall morphology. Quantitative analysis of myofiber diameter was performed by converting the image to a black-and-white image using the free software ImageJ and customized macros. The minimal Feret's diameter was analysed by computerized image analysis in 5 randomly selected fields (0.18 mm²) in 1–2 cross sections per animal. In addition, paraffin-embedded unstained sections of quadriceps were used for Second Harmonic Generation (SHG) imaging of collagen using Genesis@200 Imaging System and subsequent computer-assisted data analysis (HistoIndex Pte Ltd., Singapore). SHG is a non-linear optical process highly sensitive to non-centrosymmetric structures such as

collagen fibrils and fibers [33]. Collagen was quantified by measuring the area occupied by collagen relative to the total area of the sample (collagen area ratio).

2.4. Transcriptome analysis

RNA extraction was performed as described previously in detail [34]. Total RNA was extracted from individual liver (lobus dexter lateralis) samples (n = 10–11/group), perigonadal WAT samples (n = 8–10/group) and quadriceps (n = 7–10/group) samples using glass beads and RNA-Bee (Campro Scientific, Veenendaal, The Netherlands). RNA integrity was examined using the RNA 6000 Nano Lab-on-a-Chip kit and a bioanalyzer 2100 (Agilent Technologies, Amstelveen, The Netherlands). The NEBNext Ultra II Directional RNA Library Prep Kit (NEB #E7760S/L, New England Biolabs, Ipswich, MA, USA) was used to process the samples. Briefly, mRNA was isolated from total RNA using the oligo-dT magnetic beads. After fragmentation of the mRNA, cDNA synthesis was performed; this was ligated with the sequencing adapters and amplified by PCR. Quality and yield of the amplicon was measured (Fragment Analyzer, Agilent Technologies, Amstelveen, The Netherlands). The size of the resulting product was consistent with the expected size distribution (a broad peak between 300 and 500 bp). Clustering and DNA sequencing, using the Illumina NovaSeq6000, was performed according to manufacturer's protocols of service provider GenomeScan B.V. (Leiden, the Netherlands) using a concentration of 1.1 nM of amplicon library DNA and yielding 15–25 million sequencing clusters per sample and 2 × 150 bp Paired-End reads (PE) per cluster. The genome reference and annotation file Mus_musculus.GRCm38.gencode.vM19 was used for analysis. The reads were aligned to the reference sequence using the STAR 2.5 algorithm with default settings (<https://github.com/alexdobin/STAR>). Based on the mapped read locations and the gene annotation HTSeq-count version 0.6.1p1 was used to count how often a read was mapped on the transcript region. These counts serve as input for the statistical analysis using DESeq2 package [35].

2.5. Statistical analysis

All values shown represent means ± SEM. Statistical differences between groups were determined by using non-parametric Kruskal-Wallis followed by Mann-Whitney *U* test for independent samples using SPSS software. A p-value <0.05 was considered statistically significant. Two-tailed p-values were used. In the case of transcriptome analysis, selected differentially expressed genes (DEGs) were used as an input for pathway analysis (p-value <0.01) through Ingenuity Pathway Analysis suite (www.ingenuity.com, accessed 2020). The differentially expressed pathways (DEP) and upstream regulators were selected based on pathway enrichment (p-value Fisher's exact test) and z-score for directionality. A negative z-score < -2 indicates a predicted reduction in activity based on the direction of gene expression changes of target genes, while a positive z-score > 2 indicates activation.

3. Results

3.1. Exercise and dietary intervention have beneficial effects on body weight and metabolic plasma parameters

To induce severe obesity, insulin resistance, hyperlipidemia and inflammation, Ldlr^{-/-}.Leiden mice were fed a HFD for 50 weeks. At the start of the interventions, after 30 weeks of HFD feeding, many of these risk factors were already severely induced (Supplemental Table 1). After 50 weeks, the HFD feeding resulted in increased body weight (with +29%, p < 0.001), elevated plasma insulin (3.9-fold, p < 0.001), cholesterol (3.0-fold, p < 0.001) and triglycerides levels (2.2-fold, p = 0.001) when compared with age-matched control animals on a chow diet, while blood glucose levels remained similar (Table 1). Calorie

Table 1
Metabolic parameters.

	Chow		HFD control		Exercise		Dietary intervention		Combination	
Body weight (g)	42.3	± 1.9 ^{***}	59.7	± 0.8	48.9	± 2.0 ^{***}	46.4	± 1.3 ^{***}	40.3	± 1.9 ^{***}
Food intake (kCal/m/d)	12.6	± 0.2	15.1	± 1.0	16.1	± 0.7	13.6	± 0.4	16.2	± 0.8
Blood glucose (mM)	7.6	± 0.2	7.0	± 0.2	7.0	± 0.2	8.0	± 0.3 ^{**}	7.1	± 0.3
Plasma insulin (ng/mL)	3.0	± 0.5 ^{***}	11.7	± 1.3	16.1	± 2.2	5.1	± 0.7 ^{***}	3.0	± 0.5 ^{***}
HOMA-IR	1.0	± 0.2 ^{***}	3.7	± 0.4	5.0	± 0.6	1.8	± 0.2 ^{**}	1.0	± 0.2 ^{***}
Plasma cholesterol (mM)	10.3	± 0.9 ^{***}	30.3	± 2.2	25.0	± 1.8 [*]	13.7	± 1.2 ^{***}	8.4	± 0.6 ^{***}
Plasma triglycerides (mM)	1.9	± 0.2 ^{**}	4.2	± 0.4	3.7	± 0.4	2.6	± 0.4 ^{**}	1.1	± 0.1 ^{***}
Plasma ALT (U/L)	48.5	± 8.0 ^{***}	247.4	± 26.2	133.2	± 23.7 ^{**}	77.1	± 8.6 ^{***}	52.5	± 7.1 ^{***}
Plasma SAA (µg/mL)	9.4	± 0.5 ^{***}	21.1	± 1.0	19.2	± 2.1	11.6	± 1.1 ^{***}	11.3	± 1.7 ^{***}
Plasma E-selectin (ng/mL)	58.5	± 2.9 ^{**}	75.7	± 2.7	73.4	± 1.9	58.3	± 1.7 ^{***}	58.9	± 1.7 ^{***}
Plasma TNF-α (pg/mL)	7.1	± 1.8 ^{**}	15.0	± 2.9	8.5	± 2.1 [*]	8.2	± 1.6 [*]	4.3	± 0.5 ^{***}

Body weight, food intake and plasma parameters in *Ldlr*^{-/-}.Leiden mice fed a high fat diet (HFD) for 30 weeks and left untreated (HFD control; n = 17) or treated via administration of a running wheel (exercise group; n = 17), a switch to a healthy chow diet (dietary switch; n = 18) or the combination (combination; n = 18) thereof for 20 weeks. As a healthy reference group mice that were fed chow diet for 50 weeks were added (chow; n = 10). Values represent mean ± SEM.

* p < 0.05.

** p < 0.01.

*** p < 0.001 vs. HFD control.

intake per mouse per day was comparable between HFD and chow diet groups (Table 1) indicating that the diet change was isocaloric. Liver injury marker plasma ALT (5.1-fold, p < 0.001) and inflammation markers plasma SAA, E-selectin and TNF-α (2.3-fold, p < 0.001; 1.3-fold, p = 0.001 and 2.1-fold, p = 0.008, respectively) were all significantly elevated as well on the HFD as compared to the chow diet.

Exercise or dietary intervention during the last 20 weeks of the study profoundly curtailed weight gain, resulting in a significantly lower body weight at week 50 as compared to the HFD control group (-18% and -22%, both p < 0.001, respectively) and the combination of exercise and dietary intervention led to a significant further lowering of body weight (-32%, p < 0.001; Table 1) which was also significant compared to the mono-interventions. Exercise alone did not affect plasma insulin or blood glucose levels, while diet change significantly decreased plasma insulin levels (2.3-fold, p < 0.001) and slightly increased blood glucose levels (1.1-fold, p = 0.003) as compared to HFD control, overall resulting in a lower insulin resistance index (HOMA-IR) as compared to the HFD control group (2.1-fold, p = 0.001)(Table 1). Interestingly and despite that exercise mono-treatment did not have a significant effect, the combination of exercise and diet change resulted in a significant further improvement of plasma insulin levels and HOMA-IR (3.9-fold and 3.7-fold lowering vs. HFD control, respectively, both p < 0.001; also significant vs. mono-treatments)(Table 1). Plasma cholesterol was significantly decreased as compared to HFD control by exercise, diet change and combination thereof (-18%, p = 0.042; -55%, p < 0.001 and -72%, p < 0.001, respectively) while plasma triglycerides were not significantly affected by exercise, significantly decreased by diet change (-39%, p = 0.003) and even further decreased by the combination of exercise and dietary intervention (-73%, p < 0.001)(Table 1). Plasma ALT was significantly decreased relative to HFD control by exercise, diet change and their combination (1.9-fold, p = 0.003; 3.2-fold, p < 0.001 and 4.7-fold, p < 0.001, respectively)(Table 1). Exercise did not affect inflammation markers plasma SAA and E-selectin, but significantly decreased plasma TNF-α (-43%, p = 0.011), while the diet change significantly decreased plasma SAA, E-selectin and TNF-α (-45%, p < 0.001; -23%, p < 0.001 and -46%, p = 0.020, respectively). Combination of exercise and diet change significantly decreased plasma SAA and E-selectin (-46% and -22%, both p < 0.001), similarly as the dietary intervention alone, but led to a significant further reduction in plasma TNF-α (-71%, p < 0.001)(all Table 1).

3.2. Exercise and diet change have beneficial effects on NASH with additive effect for combination therapy on steatosis, but not for inflammation and fibrosis

HFD feeding for 50 weeks induced severe steatosis, hepatic inflammation and fibrosis in *Ldlr*^{-/-}.Leiden mice (Fig. 1A) and many of

these histological features were already fully established after 30 weeks, i.e. at the start of the intervention, as confirmed in an additional group of reference mice (Supplemental Table 1). Quantitative analysis (Fig. 1B, C) revealed that after 50 weeks about 43% of the surface area was steatotic, of which 21% consisted of macrovesicular steatosis and 22% of microvesicular steatosis. Exercise alone did not have an effect on macrovesicular steatosis, but significantly reduced microvesicular steatosis as compared to HFD control (-42%, p = 0.048). Diet change significantly reduced macrovesicular steatosis (-57% p < 0.001) and tended to reduce microvesicular steatosis as well (-32%, p = 0.087). Combination of exercise and dietary intervention led to significant further reductions of both macro- and microvesicular steatosis (-79% and -77%, both p < 0.001) indicating additive effects. Biochemical analysis of intrahepatic lipids (Fig. 1D-F) substantiated these results and revealed that the reduction in microvesicular steatosis by exercise was primarily due to a significant reduction in hepatic cholesterol esters (-13%, p = 0.023), while diet change significantly reduced hepatic triglycerides (-29%, p = 0.021) as well as hepatic free cholesterol and cholesterol esters (-18% and -51%, both p < 0.001, respectively). Combination of exercise and dietary intervention led to the largest reductions in hepatic triglycerides, free cholesterol and cholesterol esters (-60%, -25% and -63%, all p < 0.001, respectively).

HFD feeding strongly induced lobular inflammation, characterized by aggregates of inflammatory cells comprising mononuclear cells and polymorphonuclear cells. Quantification of the lobular inflammation (Fig. 1G) showed that the HFD feeding resulted in a robust increase in the number of aggregates as compared to the chow diet (31.6-fold increase, p < 0.001). Exercise intervention and dietary intervention almost fully blunted HFD-induced hepatic inflammation (-84% and -94%, both p < 0.001), and a comparably pronounced effect was observed for the combination of exercise and diet change (-95%, p < 0.001).

HFD feeding strongly induced hepatic fibrosis, as shown by collagen deposition in characteristic patch-like structures (Fig. 1A; Sirius Red staining). Quantification of liver fibrosis by computerized analysis of collagen deposition in histological slices (Fig. 1H) revealed a profound increase in collagen deposition as compared to the chow diet (3.1-fold increase, p < 0.001), a marked effect that was substantiated by biochemical analysis of collagen (Fig. 1I; 7.1-fold increase, p < 0.001). Exercise alone tended to preclude the fibrosis induction (-23%, p = 0.063 for histological collagen content and -30%, p = 0.095 for biochemical collagen content), while diet change alone significantly reduced hepatic fibrosis as compared to HFD control (-42% for histological collagen content and -61% for biochemical collagen content, both p < 0.001), and combined treatment of exercise and diet change did not further attenuate liver fibrosis (-35%, p = 0.009 for histological collagen content and -56%, p < 0.001 for biochemical collagen content).

3.3. Dietary intervention has beneficial effects on atherosclerosis with additive effect when combined with exercise

Ldlr^{-/-}.Leiden mice are hyperlipidemic mice that are known to develop atherosclerosis during aging, which can be aggravated by HFD feeding [15,21,22]. At the end of the current experiment mice on the chow diet had already developed severe atherosclerotic lesions in the aortic valve area, and the total lesion load was further enhanced by the HFD (Fig. 2A). The total lesion area in the HFD control group was 3.9-fold increased as compared to the chow fed animals (Fig. 2B). While exercise alone did not have a significant effect on atherosclerotic lesion size, diet change led to a significant reduction of the lesion area (by -20%, $p = 0.038$) and remarkably the combination of exercise and diet interventions led to a significant further reduction of lesion area (-41%, $p < 0.001$ vs. HFD control)(Fig. 2B).

3.4. Exercise and dietary intervention have beneficial effects on WAT with additive effects for combination therapy on adipocyte size, but not for WAT inflammation

HFD feeding induced obesity in Ldlr^{-/-}.Leiden mice and the lifestyle interventions resulted in slightly different effects on the various adipose tissue depots (Fig. 3A–F). Total fat mass, measured via EchoMRI, was 2.1-fold increased ($p < 0.001$) on the HFD as compared to mice on the chow diet. Exercise and diet change profoundly curtailed total fat mass, resulting in a significantly lower fat mass at week 50 as compared to the HFD control group (by -31% and -42%, both $p < 0.001$, respectively) and the combination of exercise and dietary intervention led to a significant further lowering of body weight (-69%, $p < 0.001$; Fig. 3B) (also significant as compared to the mono-interventions). Plasma leptin levels were in line with this observation and were significantly decreased for both exercise and diet change as compared to HFD control group (-31%, $p < 0.01$ and -61%, $p < 0.001$), with a further decrease for the combination treatment (-80%, $p < 0.001$)(Fig. 3C). Plasma adiponectin, often inversely correlated with fat mass [36], was indeed found to be decreased (-31%, $p = 0.011$) upon HFD feeding as compared to chow diet. Exercise alone increased plasma adiponectin levels relative to HFD control group (by +30%, $p = 0.031$), while diet change either alone or in combination with exercise did not affect adiponectin (Fig. 3D). Adipocyte size (Fig. 3E) and WAT inflammation (Fig. 3F) was quantified in both perigonadal (epididymal) and visceral (mesenteric) WAT depots. While HFD feeding did not result in a larger expansion of the adipocytes in perigonadal WAT as compared to the expansion of aging mice on the chow diet, the perigonadal fat depot had significantly more inflammation on the HFD, as shown by the increased (9.1-fold, $p < 0.001$) number of crown-like structures (CLS)/mm² perigonadal WAT. Exercise and diet change both significantly reduced perigonadal adipocyte size as compared to the HFD control group (-22%, $p = 0.002$ and -31%, $p < 0.001$, respectively), while WAT inflammation tended to be reduced with exercise (-28%, $p = 0.073$) and was significantly reduced by diet change (-37%, $p = 0.009$). While combined exercise and dietary intervention led to a significant further reduction of perigonadal adipocyte size relative to HFD control group (-46%, $p < 0.001$; also significant vs. exercise alone), inflammation in the perigonadal fat depot was not further reduced by the combination treatment (-30%, $p = 0.041$ vs. HFD control group). In case of the visceral WAT depot, HFD feeding increased adipocyte size, as well as WAT inflammation as compared to the chow group (1.3-fold, $p = 0.009$ and 3.7-fold, $p = 0.003$, respectively). Both lifestyle interventions had a similar effect as described for the perigonadal fat depot: exercise and dietary intervention both decreased visceral adipocyte size (-19%, $p = 0.023$ and -35%, $p < 0.001$, respectively), while inflammation tended to be reduced with exercise (-40%, $p = 0.089$) and was significantly reduced by dietary change (-47%, $p = 0.047$). The combination treatment again led to a significant further reduction of visceral adipocyte size (-52%, $p < 0.001$; also significant vs. each

mono-treatment), while WAT inflammation was comparably reduced (-53%, $p = 0.026$) as with the mono-treatments.

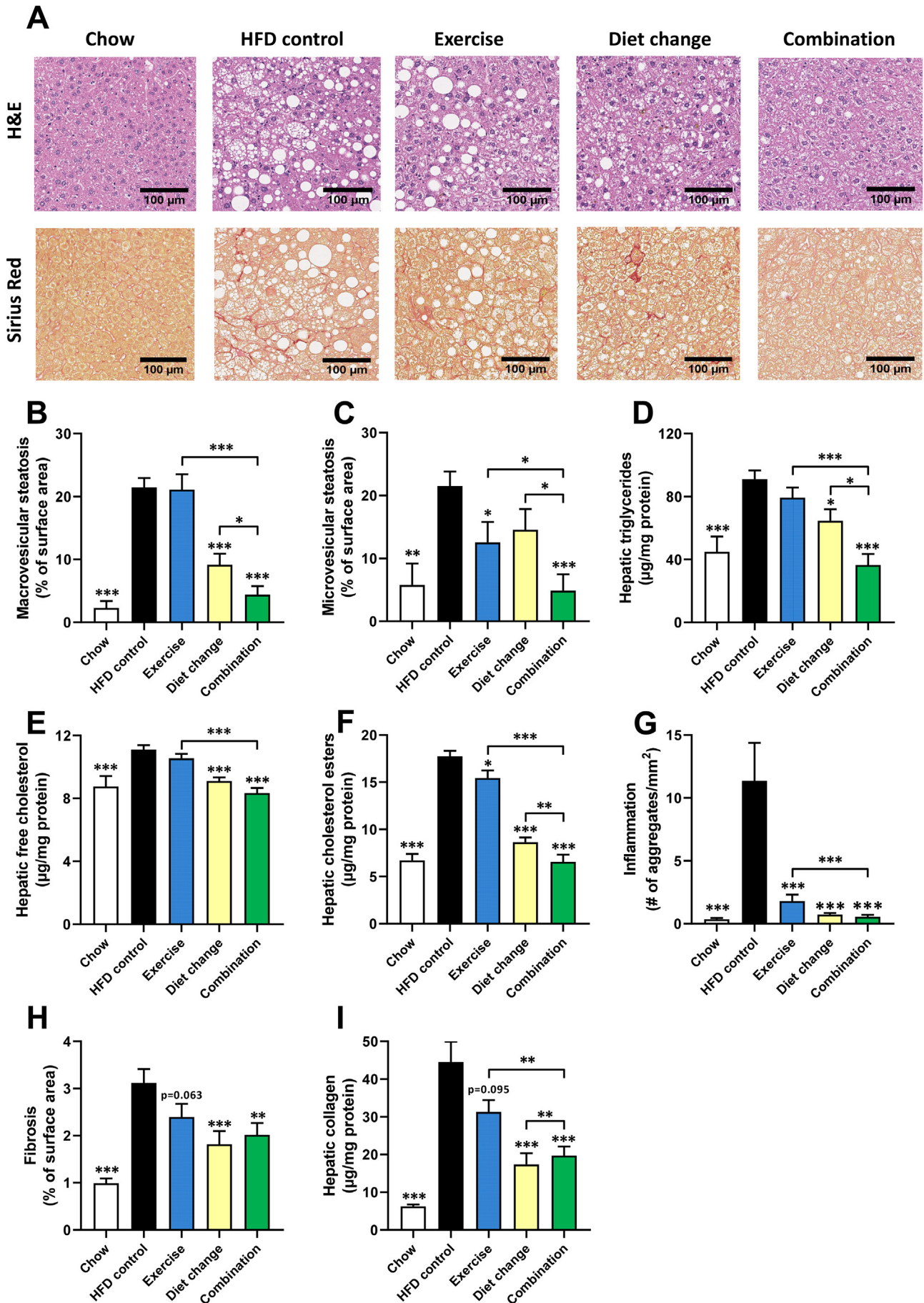
3.5. Exercise and dietary intervention have beneficial effects on muscle strength with additive effects for combination therapy

HFD feeding in Ldlr^{-/-}.Leiden mice affected muscle tissue as well (Fig. 4A–G). Absolute muscle mass (Fig. 4B) was either similar (quadriceps) in HFD group as compared to chow fed mice or tended to be increased (gastrocnemius: by +23%, $p = 0.056$). When muscle weights were expressed relative to body weight, the relative muscle mass (Fig. 4C) was however either similar (gastrocnemius) or decreased (quadriceps: by -25%, $p = 0.016$) in HFD group relative to chow mice. Both exercise and diet change significantly reduced absolute gastrocnemius weight as compared to the HFD control group (-24%, $p = 0.011$ and -20%, $p = 0.026$, respectively), while relative gastrocnemius weight or absolute and relative quadriceps weight were comparable to the HFD control group. Combination treatment led to a significant reduction in absolute gastrocnemius and quadriceps weights as compared to the HFD control group (-34%, $p < 0.001$ and -20%, $p = 0.039$, respectively). Relative gastrocnemius weight remained unchanged upon combination treatment and the relative quadriceps weight was significantly increased as compared to HFD control group (with +27%, $p = 0.004$). Muscle function was measured via four paws-grip strength (Fig. 4D) and was found to be significantly reduced upon HFD feeding as compared to the chow group (-33%, $p < 0.001$). Exercise and diet change both increased grip strength as compared to HFD control group (by +15% and +18%, both $p < 0.001$, respectively) and combination treatment resulted in a significant further increase (by +40%, $p < 0.001$). Myofiber size (Fig. 4E) was analysed by converting the image to a black-and-white image (Fig. 4A) and using the minimal Feret's diameter, as this measure of myofiber size was previously reported to be least sensitive to changes in sectioning angle [37]. HFD feeding did not affect the average minimal Feret's diameter, nor did exercise or diet change have an effect. However, the combination intervention led to a significant increase in the minimal Feret's diameter when compared to the HFD control group (43.6 ± 0.9 vs. $41.66 \pm 0.6 \mu\text{m}$, $p = 0.005$). Since muscle collagen is related to muscle stiffness, a refined analysis of collagen was performed on unstained histological cross-sections of quadriceps using SHG imaging (Fig. 4A) – which provides information on individual collagen fibrils and fibers. The area occupied by collagen relative to the total area of the sample (Fig. 4F) was increased by HFD feeding when compared to the chow group (by +45%, $p = 0.038$), but neither exercise, nor diet change, nor the combination intervention had an effect on the collagen area ratio as compared to the HFD control group. Since skeletal muscle fat accumulation has been linked to the pathogenesis and severity of NASH [38], a biochemical analysis of intramuscular triglycerides was performed on quadriceps as well (Fig. 4G) and revealed that HFD feeding strongly increased the amount of intramuscular triglycerides as compared to the chow group (by +90%, $p < 0.001$). Exercise, diet change and the combination intervention decreased intramuscular triglycerides relative to the HFD control group (-38%, $p = 0.002$; -34%, $p = 0.006$ and -59%, $p < 0.001$ respectively).

3.6. Exercise, diet change and combination intervention have differential effects on transcriptomic profile

The results from histology showed that the effects of exercise and diet change differ between organs, and the combination of both is partly of added value suggesting complementary mechanisms. To further investigate the effects on pathways, Next Generation Sequencing was performed in liver, perigonadal WAT and quadriceps muscle. Pathways that were differentially expressed by exercise, diet change or the combination thereof were compared relative to HFD control group.

Fig. 5A–C shows that the number of overlapping pathways in the intersection of exercise and diet change was relatively modest in liver,



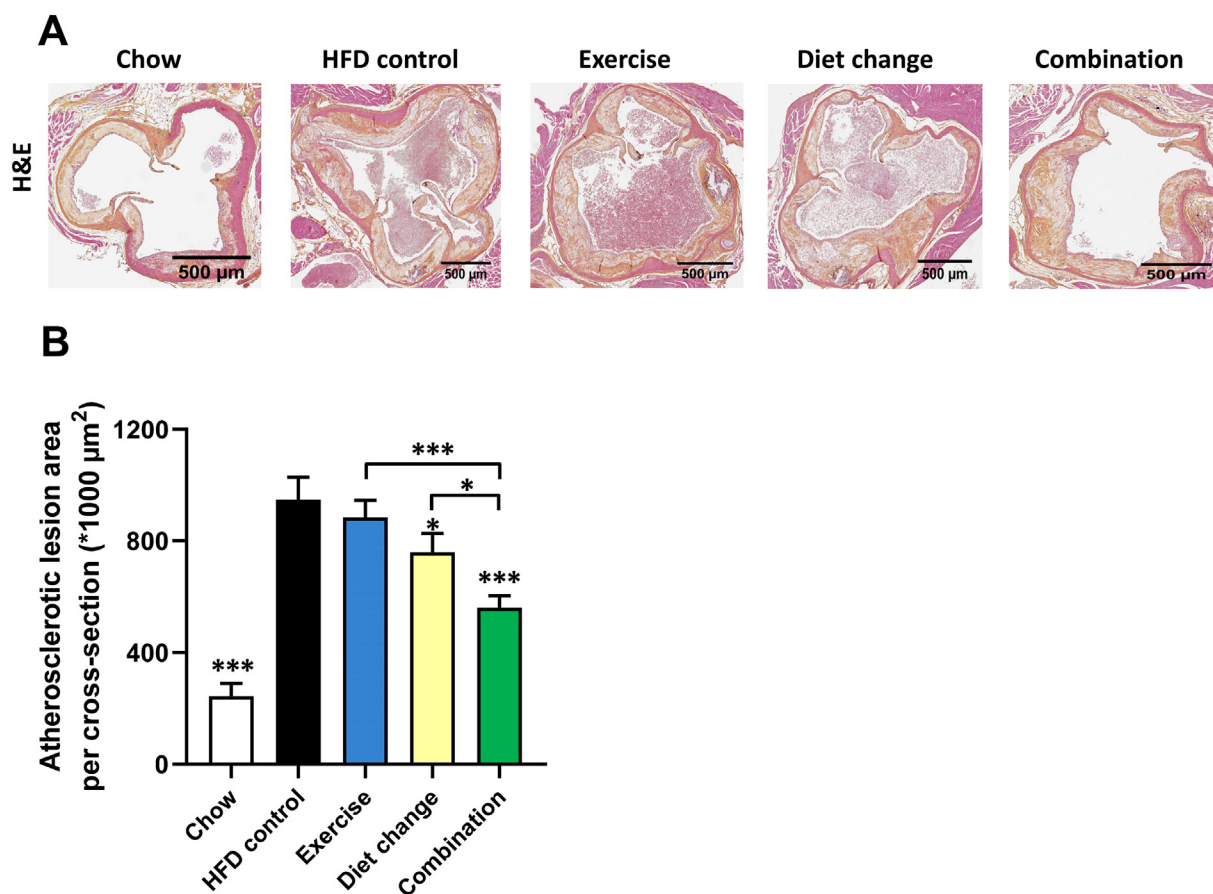


Fig. 2. Representative images of atherosclerotic plaques in aortic root section (A) stained with haematoxylin-phloxine-saffron (HPS) from *Ldlr*^{-/-}.Leiden mice fed a high fat diet (HFD) for 30 weeks and left untreated (HFD control) or treated via administration of a running wheel (exercise group), a switch to a healthy chow diet (dietary switch) or the combination (combination) thereof for 20 weeks. As a healthy reference group mice that were fed chow diet for 50 weeks were added (chow). Total lesion area per cross-section was quantified (B). Values represent mean \pm SEM for $n = 10$ chow mice, $n = 17$ for HFD control and exercise mice and $n = 18$ for dietary switch and combination mice. * $p < 0.05$, ** $p < 0.01$ and *** $p < 0.001$ vs. HFD control.

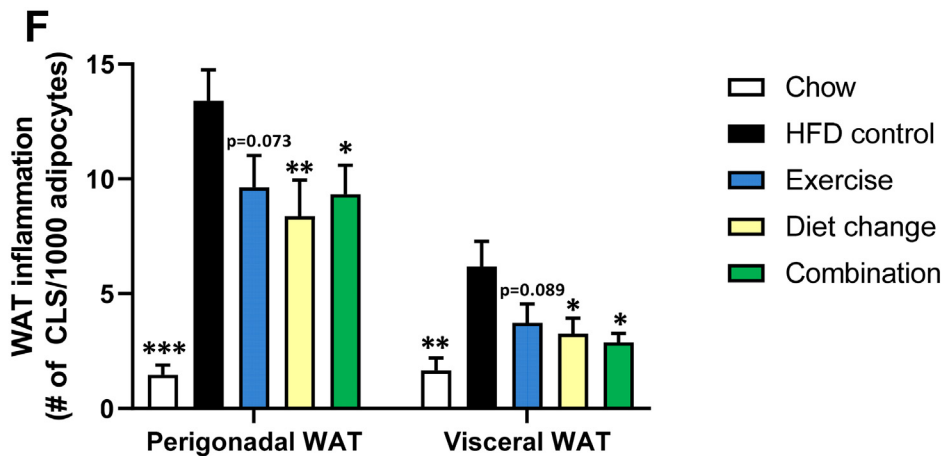
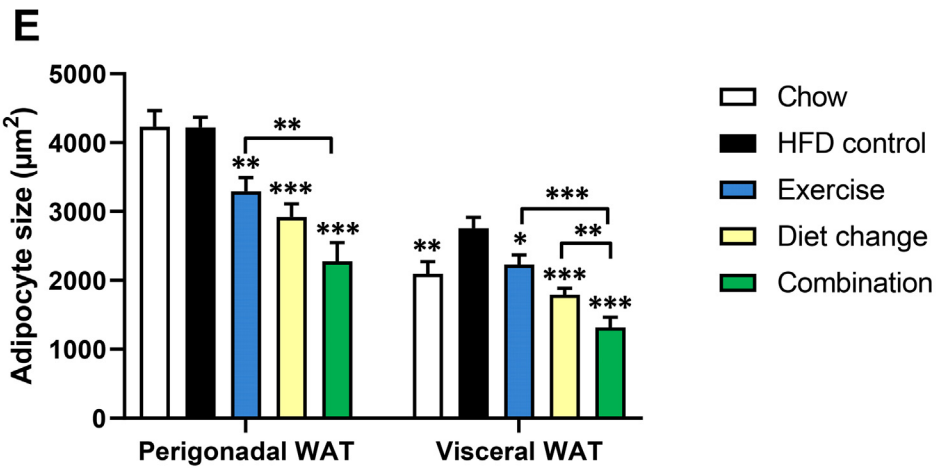
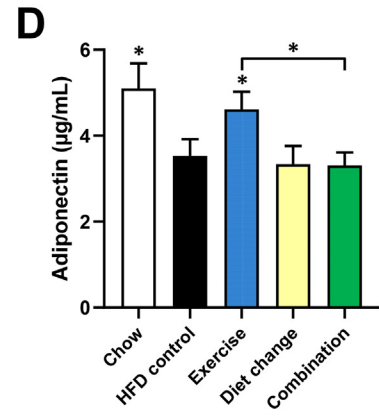
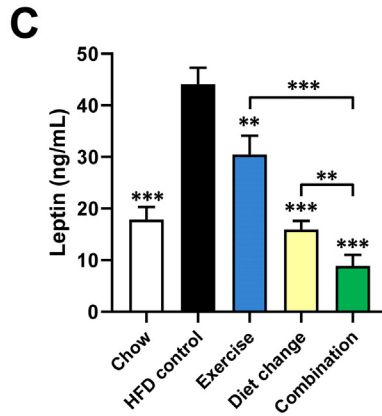
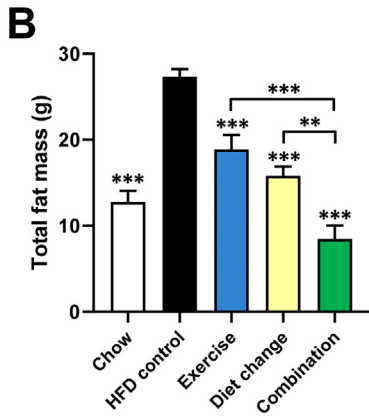
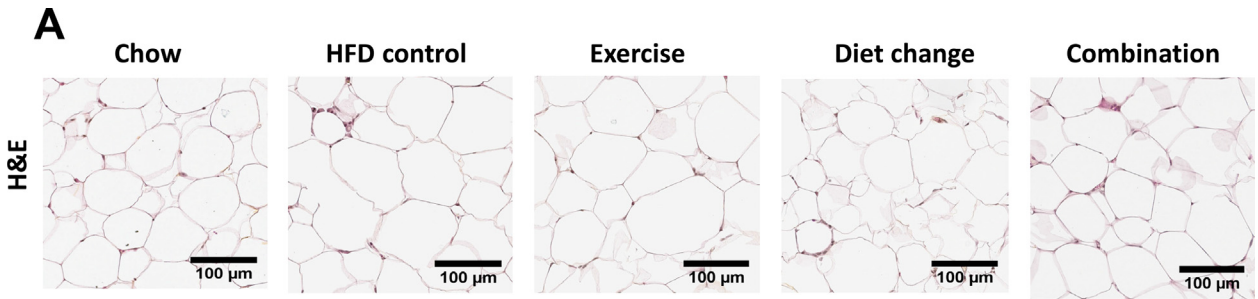
WAT and muscle indicating that the two interventions affected distinct pathways in these organs. When exercise and diet change were combined, a substantial number of new pathways became induced, in particular in WAT and muscle. These new pathways were activated at the cost of pathways from mono-treatments, demonstrating that combination therapy was not merely the sum of mono-treatments. The pathway effects will be discussed in detail per organ.

While in the liver exercise led to a total of 58 differentially expressed pathways (DEPs), diet change and combination intervention led to much more DEPs ($n = 270$ and $n = 294$, respectively), which showed great overlap (See Venn diagram in Fig. 5A). The top 15 most enriched pathways affected by exercise and diet change are shown in Fig. 5A and demonstrate that the majority of pathways affected by diet change were inflammatory pathways and pathways of cholesterol metabolism, while the pathways affected by exercise were more diverse in nature and encompassed inflammatory, cell signalling and important fibrosis pathways, like the hepatic fibrosis/hepatic stellate cell activation pathway. For the combination therapy the DEPs largely resembled the DEPs of the dietary intervention and for instance the top 15 DEPs of dietary intervention were all significantly regulated in the combination therapy as well (top 15 for combination treatment not shown),

although in a slightly different ranking. More interesting to evaluate is the additional portion of the Venn diagram, demonstrating the 51 DEPs that appear to be unique for the combination treatment. The top 15 most enriched pathways of this additional effect of combination therapy are shown in Fig. 5A and reveal several metabolism, inflammation and signalling pathways including pathways which are critical for hepatic insulin signalling (ERK pathway), inflammation and fibrosis (TNFR2 and p38MAPK pathways) and lipid homeostasis (peroxisome proliferator-activated receptor (PPAR) signalling pathway), and Type II Diabetes Mellitus signalling pathway, also an important pathway for NASH patients who are prone to develop Diabetes.

In adipose tissue, exercise and diet change affected less DEPs than in liver, in total 23 and 47 DEPs, respectively (Fig. 5B). The top 15 most enriched pathways for exercise consisted all of inflammatory pathways (including pathways related to T-cell and B-cell mediated inflammation), except for number 15, Type I Diabetes Mellitus signalling. The top 15 pathways in WAT modulated by diet change were more diverse, consisting of several inflammatory and signalling pathways, as well as fibrosis pathways, like the hepatic fibrosis/hepatic stellate cell activation pathway. The combination therapy led to a total of 92 DEPs, showed less overlap with dietary intervention in WAT than in the liver, and 65 DEPs

Fig. 1. Representative images of liver cross-sections stained with haematoxylin and eosin (H&E) or Sirius Red (A) and quantitative analysis (B-I) from *Ldlr*^{-/-}.Leiden mice fed a high fat diet (HFD) for 30 weeks and left untreated (HFD control) or treated via administration of a running wheel (exercise group), a switch to a healthy chow diet (dietary switch) or the combination (combination) thereof for 20 weeks. As a healthy reference group mice that were fed chow diet for 50 weeks were added (chow). Macrovesicular (B) and microvesicular (C) steatosis as a percentage of total liver area, biochemically analysed triglycerides (D), free cholesterol (E), and cholesterol esters (F), inflammation as number of inflammatory aggregates per mm^2 microscopic field (G) hepatic fibrosis as percentage Sirius Red of surface area (H) or biochemically analysed hepatic collagen (I). Values represent mean \pm SEM for $n = 10$ chow mice, $n = 17$ for HFD control and exercise mice and $n = 18$ for dietary switch and combination mice. * $p < 0.05$, ** $p < 0.01$ and *** $p < 0.001$ vs. HFD control.



were additionally regulated and unique for the combination therapy. The top 15 of those additional and unique pathways of combination therapy are depicted in Fig. 5B and demonstrate a mixture of inflammatory pathways (CCR5 signalling in macrophages), cancer-related and several other pathways including for NASH interesting pathways like hepatic fibrosis signalling pathway, WAT browning pathway and AMP-activated protein kinase (AMPK) signalling pathway, the latter signalling on an important cellular energy sensor that is a novel target for pharmaceutical treatment of hepatic fibrosis [39,40].

In muscle, exercise, as expected, led to the largest amount of DEPs ($n = 74$), while diet change affected 56 DEPs and the combination intervention 103 DEPs (Fig. 5C), many of which were, again, unique for the combined lifestyle treatment. The top 3 most enriched pathways induced by exercise were all related to mitochondrial functioning and the remaining pathways in the top 15 consisted of several metabolism and signalling pathways, including important pathways for muscle functioning like valine and isoleucine degradation I, tricarboxylic acid cycle (TCA) cycle II, fatty acid – oxidation I and ketolysis and ketogenesis. For dietary intervention the top 4 consisted of several inflammatory pathways, followed by several metabolism and signalling pathways including pathways such as atherosclerosis signalling and apelin adipocyte signalling (apelin being an adipokine that affects mitochondrial biogenesis via AMPK in skeletal muscle [41]), as well as key metabolism pathways like AMPK signalling and liver X receptor/retinoid X receptor (LXR/RXR) activation pathway. The DEPs of the combination intervention only partially overlapped with mono-treatments and yielded a substantial number of 50 additional DEPs unique for the combination treatment. The top 15 of these additional pathways are shown in Fig. 5C and primarily consisted of new metabolism pathways like for example gluconeogenesis I, glycolysis I, L-cysteine degradation and docosahexaenoic acid (DHA) signalling and important signalling pathways for muscle function, like actin cytoskeleton signalling and p70S6K signalling.

Notably, the top 15 pathways affected by either exercise or diet change differed for each organ indicating that exercise and diet change exerted distinct health effects in the organs investigated. Within each organ the interventions seem to complement each other because they affected many central, yet different, pathways of metabolic control, inflammation and cell signalling, the regulation of which was analysed in more detail next.

3.7. Exercise and diet change exert mechanistically complementary effects on key upstream regulators

An analysis of upstream regulators (URs) determines whether master regulators such as cytokines and their signalling receptors, enzymes or transcription factors are activated or suppressed by a treatment on basis of their downstream target genes. The top 20 consisting of the top 10 significantly up-regulated (z -score > 2) and top 10 significantly down-regulated (z -score < -2) URs for each tissue and each intervention are provided in Fig. 6.

In the liver, exercise and diet change affected many different hepatic URs critical for metabolism and inflammation and, consistent with their shared anti-inflammatory capacity they both suppressed TNF, CSF2 and IFNG signalling. Interestingly, the activities of the rate-limiting enzyme of peroxisomal beta-oxidation (ACOX1) and the fuel-sensing enzyme AMP-kinase (AMPK) were strongly enhanced by exercise indicating a normalization of energy metabolism in liver via muscle-liver organ crosstalk. Combined lifestyle intervention affected many of the URs

modulated by each of the monotreatment clearly indicating an additive effect of combined therapy, albeit the effects of diet change were more pronounced than those of exercise. Suppression of TNF, TGF β 1, CSF2, IL1 β and IFNG activities were among the top 10 URs deactivated by combination therapy which is consistent with the observed anti-fibrotic effects of the combined lifestyle treatment.

In case of adipose tissue, exercise affected markedly less URs when compared with diet change with no overlap between the top 20 URs, demonstrating that each of the monotreatment exerted distinct effects. Exercise for instance suppressed IL7 and IL12 signalling in WAT and stimulated TAF7L, a regulator of WAT formation, while diet change attenuated the activities of interferons (alpha, -beta, and -gamma), the interferon- α/β receptor (Ifnar) and interferon regulating factors (IRF3 and IRF7). In the combination therapy, the pronounced effects of diet change prevailed and overshadowed the effects of exercise.

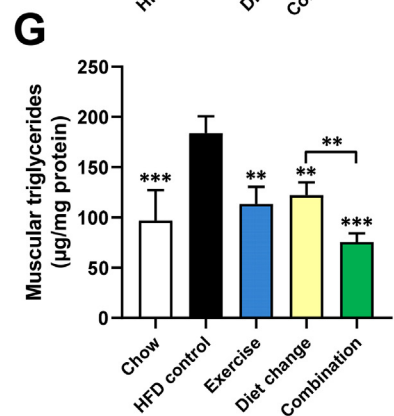
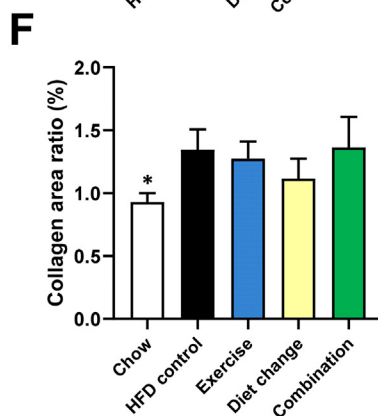
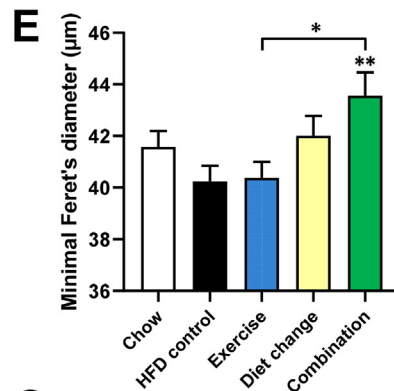
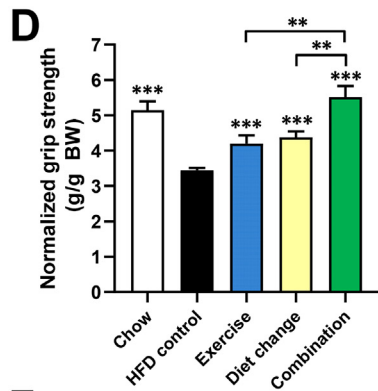
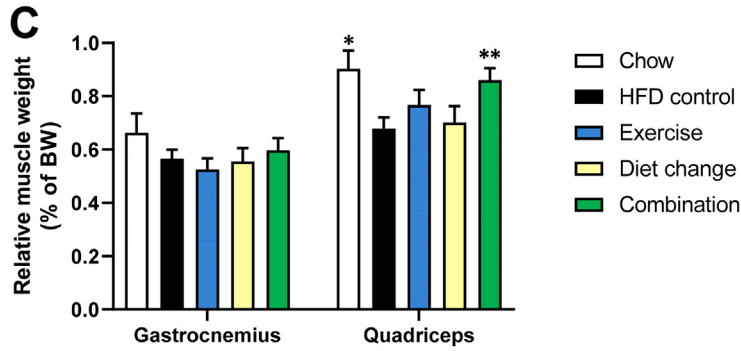
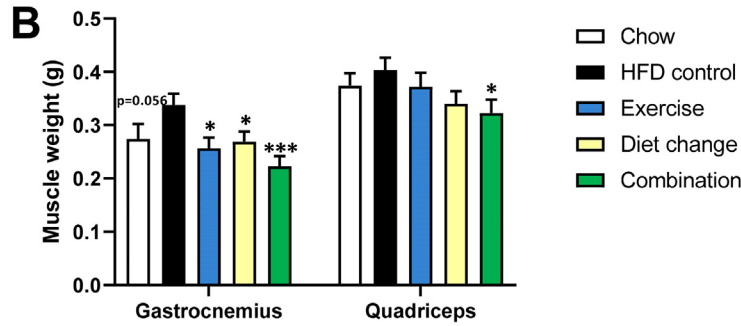
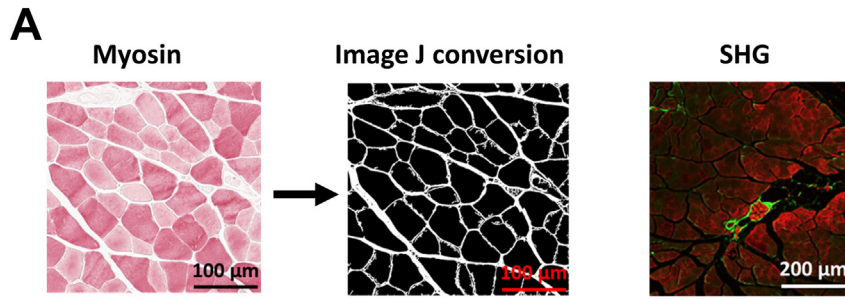
In muscle, the effects of exercise and diet change were again distinct and each treatment affected different top 10 URs. For instance, exercise strongly induced peroxisome proliferator-activated receptor- γ coactivator-1 α (PPARGC1A) activity, a master regulator of muscle health controlling mitochondrial biogenesis and anti-oxidant homeostasis [42] and insulin receptor signalling (INSR) and suppressed CEBPB, an inhibitor of myogenesis [43]. An effect specific for diet change was the suppression of interferon-alpha activity and SREBF1, a regulator of skeletal muscle cell mass and protein synthesis. The combination treatment included all of the aforementioned monotreatment effects (although not all listed in top 20) but also had some unique effects such as activation of ACOX1, the first enzyme of the fatty acid beta-oxidation (not listed in top 20).

In all, UR analysis demonstrated often quite distinct effects of exercise and diet change in the organs investigated. The effects of the two mono-treatments on a particular organ appeared to be complementary to each other, because the distinct effects from each of the monotreatment were retrieved in the combination treatment.

4. Discussion

This study in Ldlr $-/-$.Leiden mice demonstrates that lifestyle interventions, like exercise and diet change, constitute powerful treatments for already manifest and severe NASH with fibrosis. Both treatments comparably reduce body weight, however with different effects on circulating risk factors and disease endpoints indicating different modes of action. Consistent with this, combination of exercise and diet change exceeded the effect of the mono-treatments and further reduced liver steatosis including major liver lipids (hepatic triglycerides and cholesterol esters). Pre-existing hepatic inflammation was strongly resolved with both lifestyle interventions and almost completely blunted at the end of the study by all interventions. This is particularly noteworthy because the effects were very pronounced compared to reported pharmacological and nutritional treatments tested under similar experimental conditions [17,18,20,22,44,45]. Even hepatic fibrosis could be improved with lifestyle interventions further challenging current perception of disease management and the development of matrix remodelling anti-fibrotic pharmacotherapy strategies. Notably, exercise and diet change had multiple beneficial effects on distant organs and their combination further attenuated atherosclerosis, total adipose tissue mass, myosteatosis, and improved grip strength. Histological examination, as well as transcriptome analysis, of liver, WAT and muscle demonstrated exercise and diet change exerted organ-specific effects and

Fig. 3. Representative images of perigonadal white adipose tissue (WAT) cross-sections (A) stained with haematoxylin-phloxine-saffron (HPS) and quantitative analysis (B–F) from Ldlr $-/-$.Leiden mice fed a high fat diet (HFD) for 30 weeks and left untreated (HFD control) or treated via administration of a running wheel (exercise group), a switch to a healthy chow diet (dietary switch) or the combination (combination) thereof for 20 weeks. As a healthy reference group mice that were fed chow diet for 50 weeks were added (chow). Total fat mass determined by echo MRI (B), adipokines measurement of plasma leptin (C) and plasma adiponectin (D), measurement of adipocyte size (E) and WAT inflammation was analysed by measuring the number of crown-like-structures (CLS)/1000 adipocytes (F). Values represent mean \pm SEM for $n = 10$ chow mice, $n = 17$ for HFD control and exercise mice and $n = 18$ for dietary switch and combination mice. * $p < 0.05$, ** $p < 0.01$ and *** $p < 0.001$ vs. HFD control.



frequently affected distinct pathways and URs thereby providing a mechanistic rationale for the added value of the combination therapy.

Beneficial effects of exercise and diet change on NASH have been described by numerous trials and reveal that the degree of weight loss is associated with improvements in all histological NASH parameters [6,8,10]. The current evidence has led to the following guidelines from the American Association for the Study of Liver Diseases: 1) a body weight loss of 3–5% appears necessary to improve steatosis, but a greater weight loss (up to 10%) may be needed to improve necroinflammation and 2) exercise alone in adults with NAFLD may reduce hepatic steatosis but its ability to improve other aspects of liver histology (i.e. inflammation, fibrosis) remains unknown [46]. With respect to steatosis, our study results are in line with human trials because the observed weight loss of all mice with intervention correlated with their improvement in total steatosis (sum of macrovesicular and microvesicular steatosis, $r^2 = 0.56$, $p < 0.001$) indicating that more than 50% of the observed steatosis reduction may be explained by weight loss.

For hepatic inflammation, the general consensus in human trials is that a higher degree of weight loss (up to 10%) is required for improvement in hepatic inflammation. In our study (>10% body weight loss with all interventions) a more pronounced effect on hepatic inflammation was indeed observed that was profoundly curtailed by all three interventions, including exercise mono-treatment. The profound effects on lobular inflammation are remarkable and were, in particular for the exercise monotherapy, not expected because the animals still consumed HFD in comparable amounts as prior to the intervention. The top URs upregulated by exercise in the liver were acyl-coenzyme A oxidase (ACOX1) which catalyses the first step in peroxisomal beta-oxidation, AMPK, which is critically implicated in development of NASH [47] and TRIM24, an epigenetic co-regulator of transcription, which directly and indirectly represses hepatic lipid accumulation, inflammation, fibrosis and damage in the murine liver [48]. The observed exercise effects in liver are consistent with each other and together point to a normalization of hepatic energy metabolism. For all interventions, the effect size on hepatic inflammation was large and despite the smaller total range in inflammation for all interventions groups (due to this large effect size) a significant ($p = 0.009$) correlation was found between weight loss and hepatic inflammation with $r^2 = 0.13$, indicating that only 13% of the observed reduction in inflammation can be explained by the observed weight loss. At the same time, this indicates that risk factors other than body weight must have been resolved by the lifestyle interventions. Because liver inflammation in NASH has a metabolic origin and can be induced with metabolic triggers [49], one of the possible explanations could be that diet change or exercise can normalize metabolic processes at tissue level, thereby diminishing metabolic oxidative stress and associated metabolic inflammation [50]. It is thus possible that the level of tissue inflammation is predominantly determined by alterations of metabolic processes rather than a person's body weight which is also supported by the paradoxical observation that obese subjects can be relatively healthy and may exhibit low levels of tissue inflammation [51].

For hepatic fibrosis we found a significant improvement as compared to HFD control group with both diet change and combination therapy, and a trend with the exercise mono-treatment. This histological parameter was however the least affected in our study and no significant correlation was found with weight loss indicating that body weight loss does not necessarily constitute an antifibrotic effect. These findings are within expectation, since also in humans, fibrosis is a

histological NASH parameter that is not necessarily linked to obesity [52] and most difficult to improve, possibly because of the relative long half-life of collagen fibers and relative slow turn-over of matrix remodelling processes. On basis of radioactive labelling studies performed by us (unpublished), the turnover time of collagen in liver in mice is relatively long and estimated to be several months and it is well possible that a longer treatment period with exercise would have resulted in more pronounced anti-fibrotic effects. Importantly, diet change and the combination treatment both suppressed TGF- β as well as TNF- α and IL1- β , all of which critical profibrotic pathways that may explain the fibrosis-attenuating effect of diet change. Furthermore, our observation that reductions in liver fibrosis are not correlated with weight loss is consistent with human studies in which an improvement of fibrosis was found in some but not all subjects who lost more than 10% body weight [10].

When taken all data into account, the exercise mono-treatment was the least effective therapy, followed by dietary switch being more effective, and as expected, the combination therapy had the most effective beneficial effects. Interestingly, the additive value of the combination therapy became evident in all parameters related to adiposity or lipid metabolism like steatosis and muscular triglycerides, plasma lipids and atherosclerosis, as well as total fat mass and adipocyte size, while for the inflammation-related parameters this was not the case (i.e. plasma inflammation markers SAA and E-selectin, hepatic inflammation and WAT inflammation). Analysis of the underlying pathways revealed that mono-treatments of exercise and dietary change both affected numerous inflammatory pathways in liver and WAT which apparently did not always add up when the interventions were combined. Also in case of URs, the molecular effects of the mono-treatments differed in the three organs and, within each organ, they differed from each other. In all, our data supports the view that lifestyle interventions are a means to restore organ-specific pathophysiological conditions of lipid dysmetabolism and, when combined, they have added effects on endpoints associated with lipid accumulation (e.g. hepatic steatosis, myosteatorosis, atherosclerosis). It is relevant that the investigated mono-treatments affected distinct pathways that acted complementary when the therapies were combined because this provides mechanistic support to the general recommendation that an adjustment of an unhealthy diet alone is suboptimal and should be combined with greater energy expenditure via exercise, and vice versa.

In the liver exercise mono-treatment led to a relatively low amount of DEPs when compared to the dietary switch or combination treatments. Therefore, it was remarkable that hepatic inflammation was profoundly decreased by all interventions, including exercise mono-treatment. This strong effect on the liver may partially explained by organ crosstalk and the known interaction of metabolic active organs, such as liver, WAT and muscle [53]. Especially for hepatic inflammation, the contribution of inflamed WAT on hepatic inflammation is well known and the causal relationship between those tissues was for instance demonstrated by a previous experiment in which removal of inflamed WAT depot in mice led to a beneficial effect on NASH. More specifically, the induction of hepatic inflammation was hampered in the mice later in life when mice were continued on the HFD [54].

Adipokines secreted by WAT like leptin and adiponectin may play an important role in the beneficial effects on the liver. Leptin is known to affect the expression of sterol regulatory element-binding protein-1 (SREBP-1), an important transcription factor for lipogenesis in the liver [55,56], it can promote hepatic inflammation and fibrosis by enhancing the production of type 1 collagen, upregulating tissue inhibitor

Fig. 4. Representative images of quadriceps stained with anti-fast myosin immuno-staining, Image J conversion to a black-and-white image used for quantitative analysis of myofiber diameter, or unstained sections used for collagen (denoted in green) characterisation analysis via SHG imaging (A) of Ldlr-/- Leiden mice fed a high fat diet (HFD) for 30 weeks and left untreated (HFD control) or treated via administration of a running wheel (exercise group), a switch to a healthy chow diet (dietary switch) or the combination (combination) thereof for 20 weeks. As a healthy reference group mice that were fed chow diet for 50 weeks were added (chow). Absolute muscle weight (B) and relative to body weight (C), four-paw grip strength (D), average Feret's diameter as measure for quadriceps myofiber size (E), refined analysis of collagen was performed on histological cross-sections of quadriceps using SHG imaging (F) and intramuscular triglycerides determined in quadriceps (F). Values represent mean \pm SEM for $n = 10$ chow mice, $n = 17$ for HFD control and exercise mice and $n = 18$ for dietary switch and combination mice. * $p < 0.05$, ** $p < 0.01$ and *** $p < 0.001$ vs. HFD control.

of metalloproteinase (TIMP-1) and transforming growth factor (TGF)- β expression and downregulating matrix metalloproteinase 1 (MMP1) expression [57,58] and this adipokine was found to be significantly

decreased in our experiment by all three interventions. In contrast, adiponectin, an adipokine that is often inversely related to adiposity, was increased in our experiment by exercise mono-treatment only

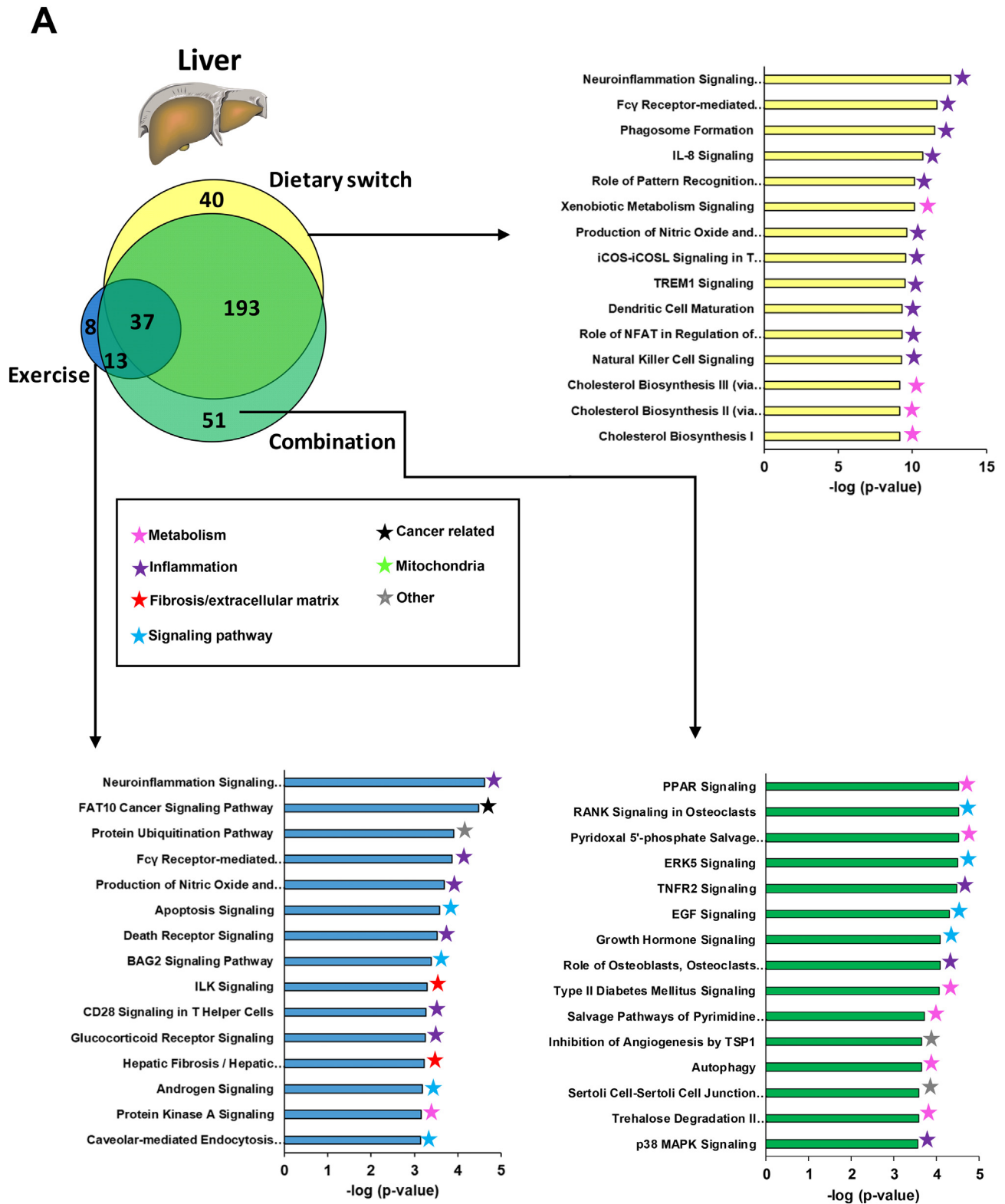


Fig. 5. Venn diagram illustrating the overlap of differentially expressed pathways in liver (A), WAT (B) or quadriceps muscle (C) between *Ldlr*^{-/-}Leiden mice receiving an exercise intervention vs. mice left untreated (blue circle), mice treated via a dietary switch vs. mice left untreated (yellow circle) or treated with the combination thereof vs. mice left untreated (green circle). $N \geq 8$ mice per group. The top 15 of significantly enriched biological processes ($-\log(p\text{-value})$) for the genes affected by exercise (blue bars) or dietary intervention (yellow bars) are shown for each tissue. For the combination treatment the top 15 of significantly enriched biological processes ($-\log(p\text{-value})$) of the additional effect or for the genes uniquely affected by the combination treatment are shown for each tissue.

B



Fig. 5 (continued).

and not by the dietary switch or combination therapy, despite the lowering of fat mass by all interventions. Since the commonality between the latter two interventions is the switch back to the chow diet, the lack of change in adiponectin levels despite the decrease in total fat mass might be related to the chow diet. The chow diet is low in fat

(9%), but relatively high in carbohydrates (58%) and it has been shown before that this can reduce plasma adiponectin levels [59].

For the pathogenesis of NASH not only the crosstalk between WAT and liver plays a role, but the crosstalk between muscle and liver has recently gained more interest as well. Skeletal muscle has been

C

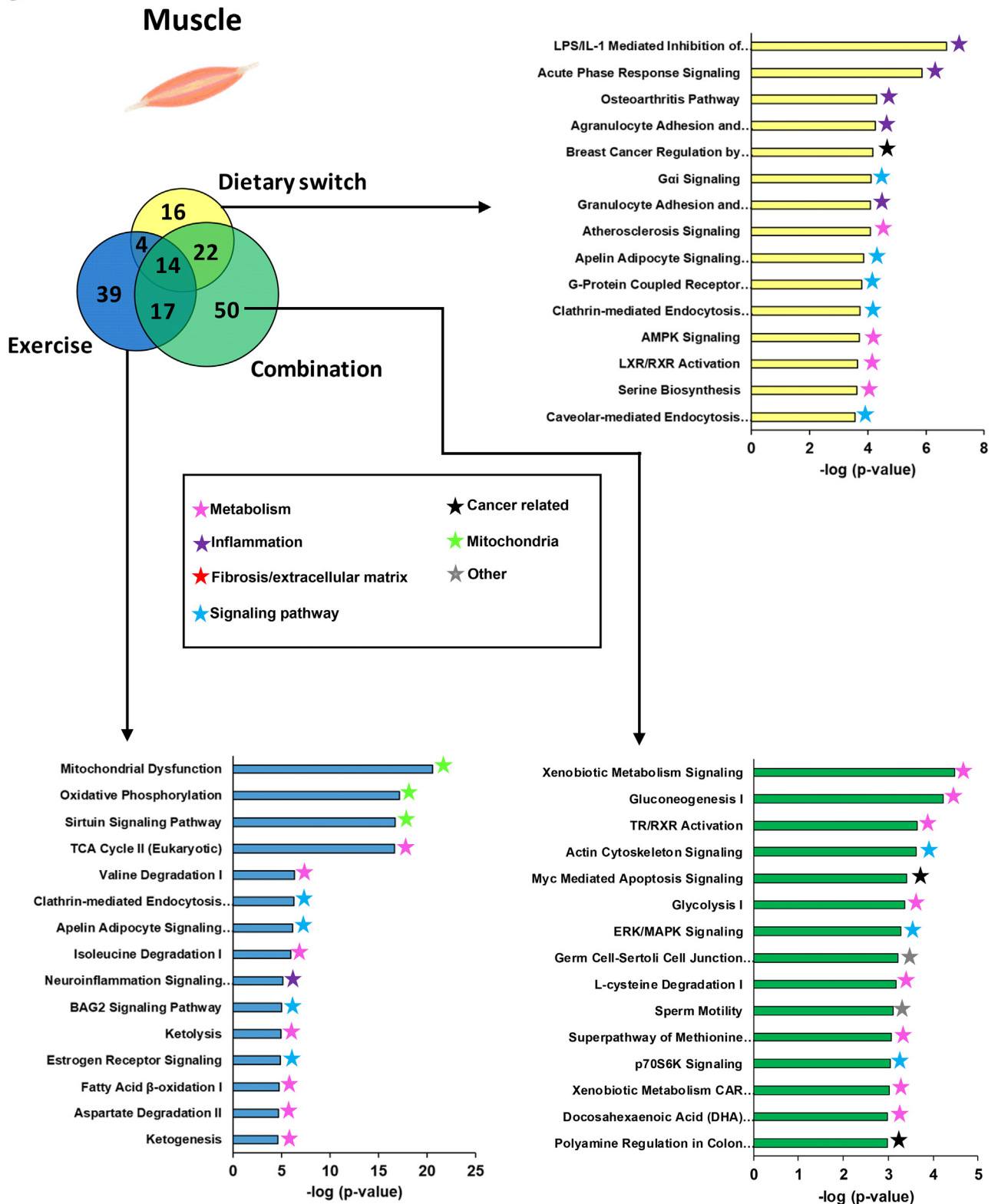


Fig. 5 (continued).

recognized as a vital organ for whole body metabolism, since it is a primary site for glucose uptake and storage, and it is also a reservoir of amino acids stored as protein [60]. However, recent studies have shown that sarcopenia, the loss of muscle mass and function, is a

novel risk factor for developing NASH and muscle, and via its impact on insulin resistance and systemic inflammation, can be of importance in NASH pathogenesis [61,62]. Not only low muscle mass, but also an adverse muscle composition comprising a high muscle fat infiltration




	Exercise			Diet change			Combination			
	Upstream regulator	Activation z-score	-log 10 overlap p-value	Upstream regulator	-log 10 overlap p-value	Upstream regulator	-log 10 overlap p-value			
	Liver	ACOX1	5.5	16.2	TRIM24	6.5	21.7	ACOX1	6.6	26.5
		TRIM24	3.2	2.9	Alpha catenin	5.5	11.1	TRIM24	6.5	11.4
		AMPK	2.9	2.0	IL10RA	5.5	27.1	Alpha catenin	6.3	12.8
		SP110	2.9	5.3	TSC2	5.4	9.3	TSC2	5.4	9.7
		ABCB4	2.4	2.4	SCAP	5.2	17.5	SCAP	5.1	11.3
		ZNF106	2.3	2.5	mir-21	4.8	17.3	Irgm1	4.8	10.8
		SMARCB1	2.2	2.4	IL1RN	4.6	6.1	ZFP36	4.7	5.7
		NCSTN	2.1	2.6	APOE	4.6	15.9	SOCS1	4.6	10.4
		SEMA7A	-2.8	4.0	ACOX1	4.4	21.0	IRF4	4.3	4.4
		HRG	-3.0	5.6	Irgm1	4.3	10.7	ABCB4	4.3	10.0
		TNF	-3.3	3.4	Ige	-6.4	24.2	IRF7	-6.8	6.0
		NFE2L2	-3.3	6.7	TGFB1	-6.4	42.4	TLR7	-6.8	4.9
		CSF2	-3.3	4.3	NFkB (complex)	-6.4	19.6	Interferon alpha	-6.8	7.7
		RABL6	-3.5	2.8	CSF2	-7.0	27.0	STAT1	-6.9	14.9
		APP	-3.6	8.1	IRF7	-7.2	19.0	IFNG	-7.2	32.9
		CSF1	-3.7	4.0	Interferon alpha	-7.4	19.9	IL1B	-7.2	23.5
		IFNG	-3.7	7.3	STAT1	-7.5	20.4	Ige	-7.4	21.7
		ERBB2	-3.8	6.4	IL1B	-7.6	25.0	CSF2	-8.2	31.2
					IFNG	-8.5	44.8	TGFB1	-8.9	44.1
					TNF	-9.1	36.2	TNF	-9.0	35.4
	WAT	TAF7L	3.2	7.0	PTGER4	4.3	8.1	AR	3.2	2.3
		NFATC1	-2.2	2.6	IL10RA	4.2	7.1	NFE2L2	3.2	3.6
		BCR (complex)	-2.5	3.0	AR	4.2	4.2	MAFB	2.8	2.5
		IL12 (complex)	-2.8	2.1	NKX2-3	4.0	2.4	PIK3CG	2.7	2.3
		TCF3	-2.8	4.4	PNPT1	4.0	9.3	MASTL	2.6	2.5
		IL7	-3.1	5.2	PIK3CG	3.9	3.9	NR1D1	2.4	3.0
		FIGLA	-3.2	7.4	ACKR2	3.6	7.3	IL10RA	2.4	11.7
					TCF7L2	3.6	2.7	FGF1	2.4	3.1
					TRIM24	3.5	10.2	CCL2_2	2.3	2.8
					SRF	3.3	2.7	SCAP	2.3	3.1
					IL27	-4.0	3.8	CIITA	-2.4	2.2
					IFNA2	-4.1	9.6	lfnar	-2.5	2.7
					miR-1-3p	-4.1	2.0	IL12A	-2.7	3.2
					PML	-4.3	3.5	EBI3	-2.7	2.6
					IRF3	-4.5	9.5	IL27	-2.8	3.8
					Interferon alpha	-4.5	8.1	IFNB1	-3.0	3.1
					IFN Beta	-4.7	6.6	TCF3	-3.0	5.9
				lfnar	-4.8	11.2	IFNG	-3.1	3.6	
				IFNG	-4.8	7.2	miR-1-3p	-3.5	3.7	
				IRF7	-5.4	14.4	IFNA2	-3.8	3.2	
	Muscle	PPARGC1A	6.9	29.7	MYCN	3.4	3.3	INSIG1	4.1	12.2
		INSR	6.1	18.6	TRIM24	3.3	3.8	miR-1-3p	3.9	6.1
		RB1	4.6	9.1	SOCS1	3.3	2.4	MYC	3.7	8.5
		MYCN	4.4	4.2	INSIG1	3.2	6.3	Alpha catenin	3.7	7.6
		PNPLA2	3.8	9.7	XDH	2.6	4.0	MYCN	3.4	3.8
		IGF1R	3.7	7.1	ZNF106	2.6	3.5	PSMB11	3.2	3.5
		NKX2-2-AS1	3.5	7.4	PNPT1	2.6	3.1	KDM1A	3.2	2.9
		INSIG1	3.4	4.4	AHR	2.6	4.7	IKZF1_2	3.1	6.7
		Alpha catenin	3.3	4.4	LDB1	2.6	5.6	RB1	3.0	3.4
		PPARD	3.2	8.9	LMO2	2.6	5.5	ZNF106	3.0	3.1
		TNFSF12	-3.6	5.8	STAT1	-3.6	9.7	TP53	-4.0	22.5
		CD44	-3.7	6.0	TNFSF11	-3.6	2.4	CD44	-4.0	6.7
		CSF2	-3.7	10.0	lfnar	-3.7	6.0	PPARA	-4.1	22.5
		ARNT2	-4.0	2.0	SREBF1	-3.7	5.5	IL6	-4.1	12.4
		TP53	-4.2	28.1	IL13	-3.9	8.2	TGFB1	-4.2	17.4
		CEBPB	-4.3	5.5	CSF2	-3.9	6.0	CG	-4.3	9.5
		RICTOR	-5.1	6.8	CD44	-4.1	9.6	TNFSF11	-4.4	4.3
		KDM5A	-5.4	17.1	PPARG	-4.1	19.3	IL13	-4.5	12.5
		MAP4K4	-5.7	18.0	IL5	-4.2	4.1	PPARG	-4.9	23.3
		CLPP	-7.1	47.2	Interferon alpha	-4.5	4.2	CEBPB	-5.0	8.3

Fig. 6. Upstream regulator analysis showing the predicted activation state (z-score) of the upstream regulators, based on the expression changes of known target genes. The overlap p-value indicates the significance of the overlap between the known target genes of a transcription factor and the differentially expressed genes measured in the experiment. Red colour indicates upregulation and blue colour indicates down-regulation. The top 10 significantly upregulated and top 10 significantly downregulated upstream regulators (if applicable, cut-off values of z-score < -2 and >2 were used) are shown for exercise, diet change and combination treatment in liver, WAT and muscle.

(myosteatorosis) is associated with the severity of NASH [38]. It has therefore been postulated that interventions that impact muscle composition and that are directed at this muscle-liver axis might be required to adequately address the pathogenesis of NASH [62]. In our current *Ldlr*^{-/-}.Leiden mouse study, we indeed observed an improved muscle composition and function with the different interventions, especially for the combination therapy, and this coincided with an improvement in the different NASH parameters and these results are therefore in line with the current notion that muscle-liver axis plays an important role in NASH pathogenesis.

5. Conclusions

In summary, *Ldlr*^{-/-}.Leiden mice were used to demonstrate that lifestyle interventions, like exercise, dietary change and the combination thereof have beneficial ameliorating effects on already preexisting NASH and liver fibrosis, demonstrating that manifest fibrosis can be treated without pharmacotherapy. In addition, the lifestyle interventions had beneficial effects on atherosclerosis, WAT inflammation and muscle function. Analysis of the underlying regulatory pathways in all three tissues revealed that while exercise and dietary change shared several underlying pathways for inflammation resulting in a net similar effect when the interventions were combined, for steatosis and other parameters related to adiposity or lipid metabolism, exercise and dietary change affected more distinct pathways that acted complementary when the interventions were combined resulting in an additive effect for the combination therapy on important endpoints including NASH and atherosclerosis. For future therapeutics, the current study advances our understanding of the development of NASH and the interaction there upon of lifestyle interventions (on a multi-organ level), and insights like these should guide the development of future pharmacotherapies.

Supplementary data to this article can be found online at <https://doi.org/10.1016/j.metabol.2021.154873>.

Funding

This work was supported in part by an allowance for TKI-LSH from the Ministry of Economic Affairs in the Netherlands (TKI Muscle Health). The authors also thank the TNO research program 'Roadmap Biomedical Health' for supporting this study.

CRediT authorship contribution statement

Anita M. van den Hoek and Robert Kleemann designed the experiments. Nicole Worms and Anita van Nieuwkoop performed the animal experiments. Jelle C.B.C de Jong, Anita van Nieuwkoop and Marijke Voskuilen performed the histological analysis on muscle, hearts and WAT, respectively, and analysed the data. Aswin L. Menke was the pathologist who performed the NASH scoring on the livers. Serene Lek carried out the muscle collagen characterisation analysis using SHG imaging. Martien P.M. Caspers and Lars Verschuren carried out the transcriptomics analysis. Anita M. van den Hoek analysed the data, prepared the figures and wrote and revised the manuscript. Robert Kleemann analysed the data, interpreted the results, and was involved in the revision of the manuscript. All authors approved the final article.

Declaration of competing interest

The authors declare no conflict of interest.

References

- Tiniakos DG, Vos MB, Brunt EM. Nonalcoholic fatty liver disease: pathology and pathogenesis. *Annu Rev Pathol*. 2010;5:145–71.
- Friedman SL, Neuschwander-Tetri BA, Rinella M, Sanyal AJ. Mechanisms of NAFLD development and therapeutic strategies. *Nat Med*. 2018;24:908–22.
- Muzurovic E, Mikhailidis DP, Mantzoros C. Non-alcoholic fatty liver disease, insulin resistance, metabolic syndrome and their association with vascular risk. *Metabolism*. 2021;119:154770.
- Polyzos SA, Kountouras J, Mantzoros CS. Obesity and nonalcoholic fatty liver disease: from pathophysiology to therapeutics. *Metabolism*. 2019;92:82–97.
- Mantovani A, Dalbeni A. Treatments for NAFLD: state of art. *Int J Mol Sci*. 2021;22.
- Hohenester S, Christiansen S, Nagel J, Wimmer R, Artmann R, Denk G, et al. Lifestyle intervention for morbid obesity: effects on liver steatosis, inflammation, and fibrosis. *Am J Physiol Gastrointest Liver Physiol*. 2018;315:G329–38.
- Promrat K, Kleiner DE, Niemeier HM, Jackvony E, Kearns M, Wands JR, et al. Randomized controlled trial testing the effects of weight loss on nonalcoholic steatohepatitis. *Hepatology*. 2010;51:121–9.
- Vilar-Gomez E, Martinez-Perez Y, Calzadilla-Bertot L, Torres-Gonzalez A, Gra-Oramas B, Gonzalez-Fabian L, et al. Weight loss through lifestyle modification significantly reduces features of nonalcoholic steatohepatitis. *Gastroenterology*. 2015;149:367–78 e5; quiz e14–5.
- Hallsworth K, Adams LA. Lifestyle modification in NAFLD/NASH: facts and figures. *JHEP Rep*. 2019;1:468–79.
- Hannah Jr WN, Harrison SA. Lifestyle and dietary interventions in the management of nonalcoholic fatty liver disease. *Dig Dis Sci*. 2016;61:1365–74.
- Priest C, Tontonoz P. Inter-organ cross-talk in metabolic syndrome. *Nat Metab*. 2019;1:1177–88.
- Muzurovic E, Mikhailidis DP, Mantzoros C. Commentary: from mice to men: in search for dietary interventions to form the background on which pharmacotherapy for non-alcoholic fatty liver disease should be based. *Metabolism*. 2020;109:154305.
- Gart E, Souto Lima E, Schuren F, de Ruiter CGF, Attema J, Verschuren L, et al. Diet-independent correlations between bacteria and dysfunction of gut, adipose tissue, and liver: a comprehensive microbiota analysis in feces and mucosa of the ileum and colon in obese mice with NAFLD. *Int J Mol Sci*. 2018;20.
- Jacobs SAH, Gart E, Vreeken D, Franx BAA, Wekking L, Verweij VGM, et al. Sex-specific differences in fat storage, development of non-alcoholic fatty liver disease and brain structure in juvenile HFD-induced obese *Ldlr*^{-/-}.Leiden mice. *Nutrients*. 2019;11.
- Luque-Sierra A, Alvarez-Amor L, Kleemann R, Martin F, Varela LM. Extra-virgin olive oil with natural phenolic content exerts an anti-inflammatory effect in adipose tissue and attenuates the severity of atherosclerotic lesions in *Ldlr*^{-/-}.Leiden mice. *Mol Nutr Food Res*. 2018;62:e1800295.
- Morrison MC, Kleemann R, van Koppen A, Hanemaaijer R, Verschuren L. Key inflammatory processes in human NASH are reflected in *Ldlr*^{-/-}.Leiden mice: a translational gene profiling study. *Front Physiol*. 2018;9:132.
- Morrison MC, Mulder P, Salic K, Verheij J, Liang W, van Duyvenvoorde W, et al. Intervention with a caspase-1 inhibitor reduces obesity-associated hyperinsulinemia, non-alcoholic steatohepatitis and hepatic fibrosis in *LDLR*^{-/-}.Leiden mice. *Int J Obes (Lond)*. 2016;40:1416–23.
- Morrison MC, Verschuren L, Salic K, Verheij J, Menke A, Wielinga PY, et al. Obeticholic acid modulates serum metabolites and gene signatures characteristic of human NASH and attenuates inflammation and fibrosis progression in *Ldlr*^{-/-}.Leiden mice. *Hepato Comm*. 2018;2:1513–32.
- Pelgrim CE, Franx BAA, Snabel J, Kleemann R, Arnoldussen IAC, Kiliaan AJ. Butyrate reduces HFD-induced adipocyte hypertrophy and metabolic risk factors in obese *LDLR*^{-/-}.Leiden mice. *Nutrients*. 2017;9.
- Salic K, Kleemann R, Wilkins-Port C, McNulty J, Verschuren L, Palmer M. Apical sodium-dependent bile acid transporter inhibition with volixibat improves metabolic aspects and components of non-alcoholic steatohepatitis in *Ldlr*^{-/-}.Leiden mice. *PLoS One*. 2019;14:e0218459.
- Schoemaker MH, Kleemann R, Morrison MC, Verheij J, Salic K, van Tol EAF, et al. A casein hydrolysate based formulation attenuates obesity and associated non-alcoholic fatty liver disease and atherosclerosis in *LDLR*^{-/-}.Leiden mice. *PLoS One*. 2017;12:e0180648.
- van den Hoek AM, Verschuren L, Worms N, van Nieuwkoop A, de Ruiter C, Attema J, et al. A translational mouse model for NASH with advanced fibrosis and atherosclerosis expressing key pathways of human pathology. *Cells*. 2020;9.
- Arnoldussen IAC, Wiesmann M, Pelgrim CE, Wielemaker EM, van Duyvenvoorde W, Amaral-Santos PL, et al. Butyrate restores HFD-induced adaptations in brain function and metabolism in mid-adult obese mice. *Int J Obes (Lond)*. 2017;41:935–44.
- Salic K, Gart E, Seidel F, Verschuren L, Caspers M, van Duyvenvoorde W, et al. Combined treatment with L-carnitine and nicotinamide riboside improves hepatic metabolism and attenuates obesity and liver steatosis. *Int J Mol Sci*. 2019;20.
- Tengeler AC, Gart E, Wiesmann M, Arnoldussen IAC, van Duyvenvoorde W, Hoogstad M, et al. Propionic acid and not caproic acid, attenuates nonalcoholic steatohepatitis and improves (cerebro) vascular functions in obese *Ldlr*^{-/-}.Leiden mice. *FASEB J*. 2020;34:9575–93.
- Post SM, de Wit EC, Princen HM. Cafestol, the cholesterol-raising factor in boiled coffee, suppresses bile acid synthesis by downregulation of cholesterol 7 α -hydroxylase and sterol 27-hydroxylase in rat hepatocytes. *Arterioscler Thromb Vasc Biol*. 1997;17:3064–70.
- Kleiner DE, Brunt EM, Van Natta M, Behling C, Contos MJ, Cummings OW, et al. Design and validation of a histological scoring system for nonalcoholic fatty liver disease. *Hepatology*. 2005;41:1313–21.
- Liang W, Menke AL, Driessen A, Koek GH, Lindeman JH, Stoop R, et al. Establishment of a general NAFLD scoring system for rodent models and comparison to human liver pathology. *PLoS One*. 2014;9:e115922.
- Delsing DJ, Offerman EH, van Duyvenvoorde W, van Der Boom H, de Wit EC, Gijbels MJ, et al. Acyl-CoA:cholesterol acyltransferase inhibitor avasimibe reduces atherosclerosis in addition to its cholesterol-lowering effect in ApoE³-Leiden mice. *Circulation*. 2001;103:1778–86.

- [30] Kuhnast S, van der Tuin SJ, van der Hoorn JW, van Klinken JB, Simic B, Pieterman E, et al. Anacetrapib reduces progression of atherosclerosis, mainly by reducing non-HDL-cholesterol, improves lesion stability and adds to the beneficial effects of atorvastatin. *Eur Heart J*. 2015;36:39–48.
- [31] Strydom HC, Chandler AB, Dinsmore RE, Fuster V, Glagov S, Insull Jr W, et al. A definition of advanced types of atherosclerotic lesions and a histological classification of atherosclerosis. A report from the Committee on Vascular Lesions of the Council on Arteriosclerosis, American Heart Association. *Arterioscler Thromb Vasc Biol*. 1995;15:1512–31.
- [32] Galarraga M, Campion J, Munoz-Barrutia A, Boque N, Moreno H, Martinez JA, et al. Adiposoft: automated software for the analysis of white adipose tissue cellularity in histological sections. *J Lipid Res*. 2012;53:2791–6.
- [33] Sun W, Chang S, Tai DC, Tan N, Xiao G, Tang H, et al. Nonlinear optical microscopy: use of second harmonic generation and two-photon microscopy for automated quantitative liver fibrosis studies. *J Biomed Opt*. 2008;13:064010.
- [34] Verschuren L, Wielinga PY, Kelder T, Radonjic M, Salic K, Kleemann R, et al. A systems biology approach to understand the pathophysiological mechanisms of cardiac pathological hypertrophy associated with rosiglitazone. *BMC Med Genet*. 2014;7:35.
- [35] Love MI, Huber W, Anders S. Moderated estimation of fold change and dispersion for RNA-seq data with DESeq2. *Genome Biol*. 2014;15:550.
- [36] Ukkola O, Santaniemi M. Adiponectin: a link between excess adiposity and associated comorbidities? *J Mol Med (Berl)*. 2002;80:696–702.
- [37] Briguet A, Courdier-Fruh I, Foster M, Meier T, Magyar JP. Histological parameters for the quantitative assessment of muscular dystrophy in the mdx-mouse. *Neuromuscul Disord*. 2004;14:675–82.
- [38] Kitajima Y, Hyogo H, Sumida Y, Eguchi Y, Ono N, Kuwashiro T, et al. Severity of non-alcoholic steatohepatitis is associated with substitution of adipose tissue in skeletal muscle. *J Gastroenterol Hepatol*. 2013;28:1507–14.
- [39] Liang Z, Li T, Jiang S, Xu J, Di W, Yang Z, et al. AMPK: a novel target for treating hepatic fibrosis. *Oncotarget*. 2017;8:62780–92.
- [40] Strzyz P. AMPK against NASH. *Nat Rev Mol Cell Biol*. 2020;21:181.
- [41] Frier BC, Williams DB, Wright DC. The effects of apelin treatment on skeletal muscle mitochondrial content. *Am J Physiol Regul Integr Comp Physiol*. 2009;297:R1761–8.
- [42] Kang C, Li Ji L. Role of PGC-1 α signaling in skeletal muscle health and disease. *Ann N Y Acad Sci*. 2012;1271:110–7.
- [43] Marchildon F, Lala N, Li G, St-Louis C, Lamothe D, Keller C, et al. CCAAT/enhancer binding protein beta is expressed in satellite cells and controls myogenesis. *Stem Cells*. 2012;30:2619–30.
- [44] Liang W, Verschuren L, Mulder P, van der Hoorn JW, Verheij J, van Dam AD, et al. Salsalate attenuates diet induced non-alcoholic steatohepatitis in mice by decreasing lipogenic and inflammatory processes. *Br J Pharmacol*. 2015;172:5293–305.
- [45] Mulder P, van den Hoek AM, Kleemann R. The CCR2 inhibitor Propagermanium attenuates diet-induced insulin resistance, adipose tissue inflammation and non-alcoholic steatohepatitis. *PLoS One*. 2017;12:e0169740.
- [46] Chalasani N, Younossi Z, Lavine JE, Diehl AM, Brunt EM, Cusi K, et al. The diagnosis and management of non-alcoholic fatty liver disease: practice Guideline by the American Association for the Study of Liver Diseases, American College of Gastroenterology, and the American Gastroenterological Association. *Hepatology*. 2012;55:2005–23.
- [47] Zhao P, Sun X, Chagga C, Liao Z, In Wong K, He F, et al. An AMPK-caspase-6 axis controls liver damage in nonalcoholic steatohepatitis. *Science*. 2020;367:652–60.
- [48] Jiang S, Minter LC, Stratton SA, Yang P, Abbas HA, Akdemir ZC, et al. TRIM24 suppresses development of spontaneous hepatic lipid accumulation and hepatocellular carcinoma in mice. *J Hepatol*. 2015;62:371–9.
- [49] Liang W, Lindeman JH, Menke AL, Koonen DP, Morrison M, Havekes LM, et al. Metabolically induced liver inflammation leads to NASH and differs from LPS- or IL-1 β -induced chronic inflammation. *Lab Invest*. 2014;94:491–502.
- [50] Hotamisligil GS. Inflammation, metaflammation and immunometabolic disorders. *Nature*. 2017;542:177–85.
- [51] Barbarroja N, Lopez-Pedraza R, Mayas MD, Garcia-Fuentes E, Garrido-Sanchez L, Macias-Gonzalez M, et al. The obese healthy paradox: is inflammation the answer? *Biochem J*. 2010;430:141–9.
- [52] Ye Q, Zou B, Yeo YH, Li J, Huang DQ, Wu Y, et al. Global prevalence, incidence, and outcomes of non-obese or lean non-alcoholic fatty liver disease: a systematic review and meta-analysis. *Lancet Gastroenterol Hepatol*. 2020;5:739–52.
- [53] Li X, Wang H. Multiple organs involved in the pathogenesis of non-alcoholic fatty liver disease. *Cell Biosci*. 2020;10:140.
- [54] Mulder P, Morrison MC, Wielinga PY, van Duyvenvoorde W, Kooistra T, Kleemann R. Surgical removal of inflamed epididymal white adipose tissue attenuates the development of non-alcoholic steatohepatitis in obesity. *Int J Obes (Lond)*. 2016;40:675–84.
- [55] Yahagi N, Shimano H, Hasty AH, Matsuzaka T, Ide T, Yoshikawa T, et al. Absence of sterol regulatory element-binding protein-1 (SREBP-1) ameliorates fatty livers but not obesity or insulin resistance in Lep(ob)/Lep(ob) mice. *J Biol Chem*. 2002;277:19353–7.
- [56] Sekiya M, Yahagi N, Matsuzaka T, Najima Y, Nakakuki M, Nagai R, et al. Polyunsaturated fatty acids ameliorate hepatic steatosis in obese mice by SREBP-1 suppression. *Hepatology*. 2003;38:1529–39.
- [57] Park HY, Kwon HM, Lim HJ, Hong BK, Lee JY, Park BE, et al. Potential role of leptin in angiogenesis: leptin induces endothelial cell proliferation and expression of matrix metalloproteinases in vivo and in vitro. *Exp Mol Med*. 2001;33:95–102.
- [58] Honda H, Ikejima K, Hirose M, Yoshikawa M, Lang T, Enomoto N, et al. Leptin is required for fibrogenic responses induced by thioacetamide in the murine liver. *Hepatology*. 2002;36:12–21.
- [59] Song X, Kestin M, Schwarz Y, Yang P, Hu X, Lampe JW, et al. A low-fat high-carbohydrate diet reduces plasma total adiponectin concentrations compared to a moderate-fat diet with no impact on biomarkers of systemic inflammation in a randomized controlled feeding study. *Eur J Nutr*. 2016;55:237–46.
- [60] Argiles JM, Campos N, Lopez-Pedrosa JM, Rueda R, Rodriguez-Manas L. Skeletal muscle regulates metabolism via interorgan crosstalk: roles in health and disease. *J Am Med Dir Assoc*. 2016;17:789–96.
- [61] Bhanji RA, Narayanan P, Allen AM, Malhi H, Watt KD. Sarcopenia in hiding: the risk and consequence of underestimating muscle dysfunction in nonalcoholic steatohepatitis. *Hepatology*. 2017;66:2055–65.
- [62] Chakravarthy MV, Siddiqui MS, Forsgren MF, Sanyal AJ. Harnessing muscle-liver crosstalk to treat nonalcoholic steatohepatitis. *Front Endocrinol (Lausanne)*. 2020;11:592373.

Supplemental Table 1: Metabolic parameters and liver histology after 30 weeks of chow or HFD as assessed in an additional group of reference mice sacrificed at the start of the intervention.

	Chow	HFD
Metabolic parameters		
Body weight (g)	35.5 ± 1.5	57.5 ± 1.0***
Blood glucose (mM)	7.4 ± 0.4	6.7 ± 0.4**
Plasma insulin (ng/mL)	2.2 ± 0.3	17.5 ± 2.2***
HOMA-IR	0.8 ± 0.1	5.3 ± 0.8***
Plasma cholesterol (mM)	6.9 ± 0.8	40.1 ± 4.8***
Plasma triglycerides (mM)	1.0 ± 0.2	8.4 ± 1.3***
Plasma ALT (U/L)	31.9 ± 1.2	457.5 ± 28.1***
Liver histology		
Macrovesicular steatosis (% of surface area)	0.2 ± 0.2	32.1 ± 1.6***
Microvesicular steatosis (% of surface area)	0.2 ± 0.1	32.8 ± 2.4***
Hepatic inflammation (number of aggregates/mm ²)	0.1 ± 0.02	9.8 ± 3.4***
Hepatic fibrosis (% of surface area)	0.6 ± 0.04	3.1 ± 1.0***